EUR 289.e

EUROPEAN ATOMIC ENERGY COMMUNITY - EURATOM

# FAST NEUTRON SPECTROMETRY IN PILE BY THRESHOLD DETECTORS

by

M. BRESESTI - A.M. DEL TURCO - A. OSTIDICH -
A. ROTA - G.J. SEGRE

1963


ORGEL Program

Joint Nuclear Research Centre
Ispra Establishment - Italy

Materials Department
Nuclear Chemistry Service

## LEGAL NOTICE

This document was prepared under the sponsorship of the Commission of the European Atomic Energy Community (EURATOM).

Neither the EURATOM Commission, its contractors nor any person acting on their behalf :

1º — Make any warranty or representation, express or implied, with respect to the accuracy, completeness, or usefulness of the information contained in this document, or that the use of any information, apparatus, method, or process disclosed in this document may not infringe privately owned rights; or

2º — Assume any liability with respect to the use of, or for damages resulting from the use of any information, apparatus, method or process disclosed in this document.

The authors' names are listed in alphabetical order.

This report can be obtained, at the price of Belgian Francs 60, from : PRESSES ACADEMIQUES EUROPEENNES — 98, Chaussée de Charleroi, Brussels 6.

Please remit payments :

— to BANQUE DE LA SOCIETE GENERALE (Agence Ma Campagne) - Brussels - account No 964.558,

— to BELGIAN AMERICAN BANK AND TRUST COMPANY - New York - account No 121.86,

— to LLOYDS BANK (Foreign) Ltd. - 10 Moorgate - London E.C.2,

giving the reference : « EUR 289.e — Fast Neutron Spectrometry in Pile by Threshold Detectors ».

Printed by Guyot
Brussels, September 1963

**EUR 289.e**

FAST NEUTRON SPECTROMETRY IN PILE BY THRESHOLD DETECTORS by M. BRESESTI - A.M. DEL TURCO - A. OSTIDICH - A. ROTA and G.J. SEGRE.

European Atomic Energy Community - EURATOM.
ORGEL Program.
Joint Nuclear Research Center - Ispra Establishment (Italy).
Materials Department - Nuclear Chemistry Service.
Brussels, September 1963 - pages 41 - figures 18.

Description is given of experiments carried out in a heavy water (Ispra 1) and a swimming pool (Avogadro RS 1) reactor.

Use has been made of detectors showing a reaction cross section of threshold type. The following reactions have been chosen : *Np*-237 (*n*, *f*); *U*-238 (*n*, *f*); *Th*-232 (*n*, *f*); *S*-32 (*n*, *p*) *P*-32; *Ni*-58 (*n*, *p*) *Co*-58; *Al*-27 (*n*, *p*) *Mg*-27; *Fe*-56 (*n*, *p*) *Mn*-56; *Al*-27 (*n*, *α*) *Na*-24.

Description is given of the methods used for the determination of the reaction rate by beta or gamma activity measurements.

**EUR 289.e**

FAST NEUTRON SPECTROMETRY IN PILE BY THRESHOLD DETECTORS by M. BRESESTI - A.M. DEL TURCO - A. OSTIDICH - A. ROTA and G.J. SEGRE.

European Atomic Energy Community - EURATOM.
ORGEL Program.
Joint Nuclear Research Center - Ispra Establishment (Italy).
Materials Department - Nuclear Chemistry Service.
Brussels, September 1963 - pages 41 - figures 18.

Description is given of experiments carried out in a heavy water (Ispra 1) and a swimming pool (Avogadro RS 1) reactor.

Use has been made of detectors showing a reaction cross section of threshold type. The following reactions have been chosen : *Np*-237 (*n*, *f*); *U*-238 (*n*, *f*); *Th*-232 (*n*, *f*); *S*-32 (*n*, *p*) *P*-32; *Ni*-58 (*n*, *p*) *Co*-58; *Al*-27 (*n*, *p*) *Mg*-27; *Fe*-56 (*n*, *p*) *Mn*-56; *Al*-27 (*n*, *α*) *Na*-24.

Description is given of the methods used for the determination of the reaction rate by beta or gamma activity measurements.

**EUR 289.e**

FAST NEUTRON SPECTROMETRY IN PILE BY THRESHOLD DETECTORS by M. BRESESTI - A.M. DEL TURCO - A. OSTIDICH - A. ROTA and G.J. SEGRE.

European Atomic Energy Community - EURATOM.
ORGEL Program.
Joint Nuclear Research Center - Ispra Establishment (Italy).
Materials Department - Nuclear Chemistry Service.
Brussels, September 1963 - pages 41 - figures 18.

Description is given of experiments carried out in a heavy water (Ispra 1) and a swimming pool (Avogadro RS 1) reactor.

Use has been made of detectors showing a reaction cross section of threshold type. The following reactions have been chosen : *Np*-237 (*n*, *f*); *U*-238 (*n*, *f*); *Th*-232 (*n*, *f*); *S*-32 (*n*, *p*) *P*-32; *Ni*-58 (*n*, *p*) *Co*-58; *Al*-27 (*n*, *p*) *Mg*-27; *Fe*-56 (*n*, *p*) *Mn*-56; *Al*-27 (*n*, *α*) *Na*-24.

Description is given of the methods used for the determination of the reaction rate by beta or gamma activity measurements.

Comparison is reported of two methods suitable for the fission rate determination.

From the activation data by different elaboration methods fast neutron distribution spectra have been calculated; a new method has been proposed.

Critical comparison of these methods has been made. The experimental data elaboration has been carried out using an IBM 7090 digital computer.

Comparison is reported of two methods suitable for the fission rate determination.

From the activation data by different elaboration methods fast neutron distribution spectra have been calculated; a new method has been proposed

Critical comparison of these methods has been made. The experimental data elaboration has been carried out using an IBM 7090 digital computer.

Comparison is reported of two methods suitable for the fission rate determination.

From the activation data by different elaboration methods fast neutron distribution spectra have been calculated; a new method has been proposed.

Critical comparison of these methods has been made. The experimental data elaboration has been carried out using an IBM 7090 digital computer.

EUR 289.e

EUROPEAN ATOMIC ENERGY COMMUNITY - EURATOM

# FAST NEUTRON SPECTROMETRY IN PILE BY THRESHOLD DETECTORS

by

M. BRESESTI - A.M. DEL TURCO - A. OSTIDICH
A. ROTA - G.J. SEGRE

1963


ORGEL Program

Joint Nuclear Research Centre
Ispra Establishment - Italy

Materials Department
Nuclear Chemistry Service

CONTENTS

## KEY TO THE FIGURES

# FAST NEUTRON SPECTROMETRY IN PILE BY THRESHOLD DETECTORS

SUMMARY

Description is given of experiments carried out in a heavy water (Ispra 1) and a swimming pool (Avogadro RS 1) reactor.

Use has been made of detectors showing a reaction cross section of threshold type. The following reactions have been chosen : *Np*-237 (*n*, *f*); *U*-238 (*n*, *f*) *Th*-232 (*n*, *f*); *S*-32 (*n*, *p*) *P*-32; *Ni*-58 (*n*, *p*) *Co*-58; *Al*-27 (*n*, *p*) *Mg*-27; *Fe*-56 (*n*, *p*) *Mn*-56; *Al*-27 (*n*, *α*) *Na*-24.

Description is given of the methods used for the determination of the reaction rate by beta or gamma activity measurements.

Comparison is reported of two methods suitable for the fission rate determination.

From the activation data by different elaboration methods fast neutron distribution spectra have been calculated; a new method has been proposed.

Critical comparison of these methods has been made. The experimental data elaboration has been carried out using an IBM 7090 digital computer.

## 1 — INTRODUCTION

1.1 The fast neutron fluxes knowledge is a question frequently proposed in reactor problems. Threshold reactions are a very useful tool in the determination of the fast neutron fluxes. Many are the advantages in using threshold detectors :

*a*) they have small dimensions and therefore they can be placed easily in the chosen irradiation positions.

*b*) they cause a negligible perturbation in the measured neutron fluxes.

*c*) their activation rate measurement is not a difficult task.

*d*) they are generally not sensible to gamma-flux apart ($\gamma$,*f*) reactions.(*)

One the other hand some difficulties must be pointed out :

*a*) the experimental data interpretation (see 1.3 and 4.).

*b*) the activation rate values may be uncorrected for contaminant activities in the target.

---

(*) The photofission cross section for *U*-238 and *Th*-232 becomes higher than 0.01 mb at about 5 *MeV* and never exceeds 10 mb (1). In that energy region, above 5 *MeV*, it is reasonable to think that the number of gamma per fission is about 1/200, and consequently that the photofission is, in this case negligible. We have not till now photofission cross sections for *Np*-237 and *Pu*-239, but it is reasonable to think that also in these cases the photofission effects are negligible.

1.2 The successful use of a threshold reaction for measuring fast neutron requires that :

*a*) the half-life of the product nucleus and the effective cross section of the parent are such to allow a suitable counting rate.

*b*) the decay scheme of the product nuclide is well known to permit an easy counting and an exact standardization.

*c*) the effect of the competitive reactions is negligible or exactly measurable.

*d*) the cross section of the reaction is a known function of the energy.

The threshold reactions used in this work are of $(n,p)$, $(n,\alpha)$ and $(n,f)$ type and are reported in table I.

*TABLE I*

| Reaction | $A^o = \int \varphi^o(E)\,\sigma(E)\,dE$ (*) | $\sigma_{eff}$ (mb) | $A^o/\sigma_{eff}$ | $E_{eff}$ |
|---|---|---|---|---|
| *Np*-237 $(n,f)$ | $1174. \times 10^{-27}$ | 1 450 | 0.809 | 0.68 |
| *U*-238 $(n,f)$ | $312. \times 10^{-27}$ | 580 | 0.538 | 1.48 |
| *Th*-232 $(n,f)$ | $71.9 \times 10^{-27}$ | 140 | 0.513 | 1.56 |
| *S*-32 $(n,p)$ *P*-32 | $65.7 \times 10^{-27}$ | 308 | 0.213 | 2.99 |
| *Ni*-58 $(n,p)$ *Co*-58 | $110. \times 10^{-29}$ | 550 | 0.200 | 3.09 |
| *Al*-27 $(n,p)$ *Mg*-27 | $3.83 \times 10^{-27}$ | 80 | 0.0385 | 5.46 |
| *Fe*-56 $(n,p)$ *Mn*-56 | $0.953 \times 10^{-27}$ | 50 | 0.0190 | 6.42 |
| *Al*-27 $(n,\alpha)$ *Na*-24 | $0.580 \times 10^{-27}$ | 70 | 0.00828 | 7.52 |

(*) - $\varphi^o(E) = 0\,.\,483\,e\,.^{-E}\,sh\,\sqrt{2E}$ (watt)

Fig. 1 and 2 show the cross section vs. neutron energy curves for the used threshold reactions. The values have been taken from BNL 325 - 2nd Edition and from a compilation of H. Liskien and A. Paulsen (2).

When different data are available from the same reaction, average values have been used. In the energy ranges, where experimental data are not available, values obtained by interpolation have been used.

Recently a collection of threshold detector cross section has been published by R. Beaugé (3) for account of the Euratom Dosimetry Group. This collection was not used in the present work being posterior to the data elaboration.

1.3 The experimental data obtained by threshold detector measurements may be expressed in the form :

$$A_i = \int \varphi(E)\,\sigma_i(E)\,dE \qquad (1)$$

indicating the reaction probability per second for one nucleus of *i-th* isotope in the differential neutron flux $\varphi(E)$.

In fact $A_i$ is the experimental value obtained by

$$A_i = \frac{D_i \, e^{-\lambda_i t_2}}{N_i \, (1 - e^{-\lambda_i t_1})} \tag{2}$$

where

$D_i$ = activity (dis/sec) of the reaction product

$\lambda_i$ = decay constant of the reaction product

$t_1$ = irradiation time

$t_2$ = cooling time

$N_i$ = target atom number

When n-threshold detectors are used, there are n-integral equations (1) where $\varphi(E)$ is the unknown differential flux.

The resolution of equations like (1) is not possible without assumptions on $\varphi(E)$.

Several methods were proposed for the solution of (1).

A survey of these devices is reported in section 4.

## 2 — EXPERIMENTAL

### 2.1 — Irradiation facilities

Measurements were carried out in the Ispra 1 and Avogadro RS I reactors. The Ispra 1 is a heavy water moderated and cooled reactor using 90 % enriched uranium fuel with a graphite reflector (CP 5 type). Avogadro RS I is a swimming pool reactor fuelled with 20 % enriched uranium.

The positions used for the sample irradiation are :

*in the Ispra 1 reactor* the PH 3 pneumatic tube and the 8 positions of the 4 DH 1 facility (fig. 3).

*in the Avogadro RS 1 reactor* the channel *D* 3 in the reactor core (fig. 4) : the samples were placed in a vertical assembly of 4 cylindrical graphite blocks. Each block, 6.8 cm in diameter and 10.5 cm high, has 7 irradiation positions. The 9 positions in which samples were irradiated are shown in fig. 5.

The samples were irradiated into 3 types of containers according to the irradiation positions.

*a*) For the pneumatic tube the targets were located into a "VITON" (rubber) cylindrical container (useful dimension : 60 mm high × 24 mm in diameter).

*b*) For the 4 *DH* 1 facility were used aluminum spherical containers $\varnothing_{int} = 28$ mm.

*c*) For the irradiations in the Avogadro *RS* 1 reactor the samples were put into quartz containers.

All the irradiations were made under 1 mm of cadmium in order to decrease the rate of $(n,\gamma)$ and $(n,f)$ reactions on the impurities of the sample.

Fig. 6 shows the VITON, aluminum and cadmium containers.

## 2.2 — Target preparation

For the irradiations only solid targets were used : high purity metal discs or high purity salts.

The salts were irradiated as powders or as thin layers on platinum discs. These thin layers were obtained by drop evaporation or by electrolytic deposition.

## 2.3 — Source preparation

For the measurements of the induced activity the following types of sources were used :

*a*) Target not handled

*b*) Suitable reaction product separated by chemical methods (in liquid or solid state).

The sources were always prepared in a geometrical form apt to the used detector.

## 2.4 — Radiation detectors

In this work the following radiation detectors were used :

*a*) A Geiger Müller counter with thin window for beta rays.

The counter efficiency was previously determined by standard sources.

*b*) A 3" × 3" *NaI* (*Tl*) scintillation spectrometer for gamma rays. This detector (an integral line produced by Harshaw Co.) was operating in connection with a 256 channels pulse analyzer and was shielded by 10 cm *Pb* (fig. 7).

This detector was calibrated for suitable solid or liquid sources and for several distances using isotopes standardized by *4pi* beta-gamma coincidences.

The photoefficiency curves are reported in fig. 8 - *a*) and *b*).

*c*) A *2pi* proportional counter for alpha particles.

*d*) A gridded ionization chamber for alpha pulse analysis.

*e*) Two 40 $mm^2$ and 200 $mm^2$ superficial barrier solid state detectors for alpha pulse analysis prepared by the Nuclear Chemistry Laboratory of Ispra.

## 2.5 — Catcher method

### 2.5.1 — *Fundamentals*

In the other methods the threshold detectors fission rate is measured by determination of the activity of one fission product of known yield and decay scheme.

In this work we have also used the catcher method in which the fission rate is measured by comparison of the total gross gamma activity of the fission products originated in threshold detectors and the same kind of activity originated in the thermal fission of *Pu*-239.

The reliability of the method is based on the validity of the following fundamental hypothesis :

— the gross gamma activity of the fission products of the threshold detectors and that of *Pu*-239 fission products follow the same decay law, in the first 3 hours after the end of the irradiation, being the irradiation and counting conditions the same.

The validity of this law has been experimentally checked by some authors (4, 5, 6) and also in the present work (see 3.4). Due to the presence of the gamma activity of the not fissioned atoms and of the $(n,\gamma)$ reactions on the fissionable atoms, it is not convenient to count with the fission products, all the irradiated material. In order to avoid the above difficulty and an eventual chemical separation, it has been therefore proposed to catch the fission products containing the source on a suitable material and to stop the $(n,\gamma)$ reactions recoils by an absorber located between the source and the catcher.

The effect of the gamma activity from $(n,\gamma)$ reaction on the monitor is particularly disturbing in the case of *Np*-237, due to the $E\gamma \sim 1\ MeV$, the $T_{1/2} \sim 2.1d$ and the high production cross section of *Np*-238.

2.5.2 — *Irradiation geometry*

The fissionable material, deposited on a *Pt* disc 17 mm in diameter, is subsequently covered by :

— *Al* foil of 0.3 mg/cm² sup. dens. to stop( $n,\gamma$) reaction recoils;

— *Al* catcher of 7 mg/cm² sup. dens. to stop the fission products;

— two *Al* catchers identical to the first one to allow the subtraction of the activity produced by the irradiation in catcher material itself.

The whole is contained in an *Al* capsule keeping all the foils adherent and covered by 1 mm of *Cd*.

The effect of the absorber on the *Np*-238 recoils is shown in fig. 9.

It is possible to see that :

— The *Np*-238 activity is only present in the absorber (fig. 9-1, 9-2).

— The 850 *KeV* accompaining the *Np*-238 activity is surely originated from a fission product with half-life inferior to that of *Np*-238.

In fact (fig. 9-1) it is stopped in the first catcher and (fig.9-3) the gamma spectrum of the absorber about 12 hours after the irradiation does not show any important activity besides that of *Np*-238.

— The percent of fission product gamma activity with $E\gamma > 0.661\ MeV$ stopped in the absorber about 1 hour after the irradiation is about 6 %. — This value is obtained from the ratio of the areas under fig. 9-1 and fig. 9-2 with $E\gamma > 0.661\ MeV$.

This value agrees reasonably with that reported by ref. (6).

An exploded vision of the irradiation device is shown in fig. 10.

2.5.3 — *Catcher materials*

An experimental study has been carried out in order to choose the best material to be used.

A perfect catcher should have the following properties :

— no activity induced by neutrons

— good foils homogeneity

— no heating deformation (heating due mainly to the capture gammas of *Cd*)

— no neutron absorption

In the following table are shown the materials checked and their properties. The activation is compared with that of the same mass of electrolytic high purity aluminum.

*TABLE II*

| Material | Activation $\gamma \geqslant 661$ *KeV* * | Heating deformation | Homogeneity of foils |
|---|---|---|---|
| graphite | 5 | no | bad |
| nuclear graphite | 1 | no | bad |
| colloidal graphite | 2 | no | not very good |
| teflon | 50 | no | good |
| polythene | 0.5 | yes | good |
| lead electrolytic | 0.1 | ? | difficult to obtain |

* Irradiation time : 10 min.; cooling time : 1 h.

The material we have chosen is the electrolytic high purity aluminum. If obtainable in thin homogeneous foils, the best material seems to be the electrolytic lead.

2.5.4 — *Irradiation and counting*

A 10 minutes irradiation time has been chosen for the following reasons :

1) to avoid the predominancy of long lived fission products.

2) a shorter irradiation time would produce an insufficient activity in our experimental conditions.

3) a shorter irradiation time would require deposits too thick for : penetrability of fission products, alpha standardization of deposited material, homogeneity of the deposit.

4) a longer irradiation time would increase the interfering activity of *Na*-24.

The gamma activity of the catcher foils with and without fission products were counted by a 3" × 3" *Na I* (*Tl*) scintillation crystal.

The integral counting is characterized by an energy cut off : in order to have a constant reference and to eliminate the disturbing low energy activities and background, a 661 *KeV* (*Cs*-137) cut off was used in all the experiments.

2.5.5 — *Fission rate determinations*

Following the hypothesis reported in 2.5.1 it is possible to determine the fission rate $A_i$ by the equation :

$$\frac{C_i}{C_{Pu}} = \frac{N_i A_i}{N_{Pu} \Phi_{th} \sigma_{Pu}}$$

where :

— $C_i$ = gamma-counting ($E > 661$ *KeV*) on the fission products stopped in the catcher foil

— $C_{Pu}$ = idem for *Pu*-239

— $N$ = number of fissionable nuclides

— $\Phi t_h$ = thermal neutron flux

— $\sigma_{Pu}$ = thermal *Pu*-239 cross section.

2.5.6 — *Comparison between fission rate determination methods*

The catcher method is affected by the following sources of error :

1) Subtraction of the catcher activity. — It depends on the ratio between the catcher and catched activities. In our experiments this type of error ranges from about 0.2 % for *Pu*-239 to about 1-2 % for *Th*-232.

2) Thermal flux and *Pu*-239 thermal activation determination. The amount of this type of error is estimated about 4 %.

3) Assumption of the equality of the decay laws. This assumption is verified, in the experimental errors, for the first two hours after irradiation. At the third hour the law is still verified for *Th*-232 and *U*-238 compared to *Pu*-239 while for *Np*-237 a deviation larger than the experimental errors was found.

The *La*-140 counting method (see § 3) is affected mainly by the followirg sources of error :

1) uncertainty on the *Ba*-140 fission yield. These uncertainties are rather high (see § 3).

2) uncertainty of the *La*-140 decay scheme, and particularly on the percentage of 1.6 *MeV* gamma-ray. (Estimated error 2 %).

3) efficiency of gamma measurements i.e. determination of photopeak efficiency and area. The amount of this error is of the order of 1-2 %.

It has to be reminded that, while in the catcher method the same target can be used many times due to the little consumption of fissionable atoms in each irradiation (about $10^{-6}$ %) this is not the case for the *La*-140 method.

An examination of the above considerations leads to prefer the catcher method. However this method presents two weak points :

— the irradiation times must be short; the exact knowledge of these times requires therefore the use of an irradiation facility like a pneumatic rabbit.

— the activity measurements must be carried out in the first 3 hours after the end of the irradiation and begin as soon as possible.

## 3 — ACTIVATION MEASUREMENTS

### 3.1 — Np - 237(n,f)

*a*) Target : *Np* nitrate solution (6 mg) deposited on aluminum foils. Irradiation time several hours. The solution was previously standardized by *4pi* alpha counting.

Some purity tests were performed on the solution : sources obtained by electrodeposition were analyzed by ionization chamber and solid state detectors.

Fig. 11*a* shows a typical spectrum of the solution and the presence of *Pu*-239 (0.43 nuclei %) and *Am*-241 (about $10^{-4}$ nuclei %) impurities.

In order to avoid a wrong value of the *Np*-237 fission rate due to the presence of *Pu*-239, a separation of *Np*-237 from *Pu*-239 was carried out by solvent extraction (TTA).

Fig. 11*b* shows a typical spectrum of the purified solution (*Pu*-239 $< 10^{-3}$ nuclei %). The *Am*-241 impurity does not introduce an error in the measurements because the quantity is too small and the cross-section too low.

*b*) Chemical separation : after the irradiations two methods were used for the sources preparation :

*b*. 1) the target and the aluminum were dissolved in 6 *N HCl* and counted as a liquid source (standard volume 5 ml).

*b*. 2) the target and aluminum were dissolved with 6 *N HCl* and *Ba*-140 was separated by carrier precipitation of $BaCl_2$ by *HCl*-ether reagent (7). $BaCl_2$ was counted as liquid source (standard volume 5 ml). Assumed fission yield of *Ba*-140 5 % (8, 9).

This figure is affected by an error of 7 %.

*c*) Counting : the *Ba*-140 (12.8 days half-life) activity was determined by counting the 1.6 *MeV* gamma photopeak of the daughter *La*-140 (40 hours half-life) (0.96 ± 0.02 gamma/dis.) :

— at least 10 days after the end of the irradiation to reduce the activity of the short-lived fission products (see *b*. 1)

— at least 134 hours after the separation (see *b*. 2).

*d*) Remarks : the activity produced by the competitive reaction *Np*-237 $(n, \gamma)$ *Np*-238, does not interfer with the measurements. In fact this gamma activity, very intense at the irradiation end, decays sufficiently rapidly (*T1/2*= 2 *d*) and its energy (about 1 *MeV*) does not disturb the 1.6 *MeV* gamma-photopeak detection. The first irradiations were carried out using unpurified solution.

The *Pu*-239 impurities fission rates were evaluated and the results were corrected.

### 3.2 — U - 238(n,f)

*a*) Target : depleted uranium in metallic form (about 10 mg) containing 350 *ppm* of *U*-235 packed in aluminum foils.

Irradiation time : several hours.

*b*) Chemical : after the irradiations the sources were prepared by the same methods used for *Np*-237.

Fission yield of *Ba*-140 5.7 %, error not given (10).

*c*) Counting : see 3.1 - *c*).

*d*) Remarks : the epithermal fission rate of *U*-235 impurities was determined by comparison of depleted and natural uranium fission rates. The *U*-238 fission rates were then suitably corrected.

### 3.3 — Th - 232(n,f)

*a*) Target : high purity thorium metal (about 20 mg) packed in aluminum foils.

Irradiation time : several hours.

*b*) Chemical : after the irradiations the sources were prepared by the same method used for *Np*-237 and *U*-238.

Fission yield of *Ba*-140 6.2 % (11).

*c*) Counting : see 3.1 - *c*).

*d*) Remarks : the *Ba*-140 fission yield for *Th*-232 is badly known. The only value reported is 6.2 ± 2.0 (11).

### 3.4 — Catcher method for Np, U, Th reactions

*a*) Target preparation. Deposition by micropipette on *Pt* backing, evaporation by infrared lamp and calcination for 30' of the deposited materials.

*b*) Target standardization. By measurements of the total alpha activity in a $2\pi$ counter. A spectroscopic study was previously carried out in order to determine the ratio between the alpha activity of the monitor and of the other alpha emitters present in the deposit (see fig. 12).

*TABLE III*

| Monitor | Temp. of calcin. (°C) | Sup. dens. ($\mu g/cm^2$) | Total $\alpha$ (dis/sec) | Other $\alpha$ emitters | $\frac{\alpha\text{-other}}{\alpha\text{-total}}$ |
|---|---|---|---|---|---|
| *Th*-232 | 500 | 2000 | 60 | daughter of *Th* | 0.76 |
| *Np*-237 | 900 | 150 | 6000 | *Pu*-239 | 0.285 |
| *U*-238 | 800 | 500 | 10 | *U*-235 *U*-234 | $6.75 \times 10^{-2}$ |
| *Pu*-239 | 1000 | 1 | 2000 | *Am*-241 | 21.9 |

In the last experiences *Np*-237 separated from *Pu*-239 was used. The *Pu*-239 presence, in fact, produces a hardly figurable error due to its high fission cross section.

The calculated absorption of the alpha particles emitted and of the fission products in the deposits is of the same order of magnitude. It therefore follows that the error of neglecting the alpha autoabsorption in the sources is compensated by neglecting the fission products absorption in the sources.

*c*) Test of the fundamental hypothesis.

In fig. 13 is shown an example of *Th*-232, *U*-238, *Np*-237, *Pu*-239 fission products with $E > 0.661\ MeV$, gamma decay. See some remarks about this matter at 2.5 - *f*).

### 3.5 — S - 32(n,p) P - 32

*a*) Target : high purity $MgSO_4$ (about 100-200 mg) in aluminum cans.

Irradiation time : several hours.

*b*) Chemical : after the irradiations two methods were used for the sources preparation.

*b*. 1) $MgSO_4$ was dissolved in water; carrier-free *P*-32 was separated by adsorption on an alumina column and elution with $0.5N\ NaOH$ - $Na^+$ ions were eliminated by adsorption on a cationic resin (12).

A known amount of the solution containing only carrier-free *P*-32 was then deposited by drop evaporation on metallic discs and counted.

*b*. 2) $MgSO_4$ was dissolved in water.

An amount of solution containing 0.5 mg of salt was deposited by drop evaporation on metallic discs and counted.

*c*) Counting : the $\beta^-$ activity of *P*-32 ($E_{max} = 1.71\ MeV$) was determined by a Geiger-Müller counter calibrated :

— with sources of *P*-32 carrier-free (see 3.5 - *b*. 1) standardized by $4pi\ \beta^-$ counter.

— with sources of *P*-32 carrier-free standardized by $4pi\ \beta^-$ counter + 0.5 mg $MgSO_4$ (see 3.5 - *b*. 2).

In the second case the sources were counted with 55 mg/cm² aluminum absorber to eliminate *S*-35 $\beta^-$ activity.

The $\beta^-$ activity purity was controlled by following the beta decay.

*d*) Remarks : the competitive reactions *S*-34$(n,\gamma)$*S*-35 and *S*-33$(n,p)$*P*-33 do not interfer with the measurements. In fact the *S*-35 $\beta^-$ activity ($E_{max} = 0.177\ MeV$ - 88 days half-life) is eliminated in the first method by chemical separation and in the second method by counting under 55 mg/cm² *Al*-absorber. The *P*-33 $\beta^-$ activity ($E_{max} = 0.250\ MeV$ - 25 days half-life) is low (about 0.5 % of the *P*-32 activity).

The $(n,\gamma)$ and $(n,p)$ activation products of magnesium, mainly *Mg*-27 (9.5 min. half-life) and *Na*-24 (15 hours half-life), were eliminated by chemical separation (see *b*. 1) or decay (see *b*.2).

### 3.6 — Ni - 58(n,p) Co - 58

*a*) Target : high purity nickel metal disc (about 100 mg) in aluminum cans.
Irradiation time : several hours.

*b*) Chemical : after the irradiation no chemical treatment was carried out on the sample.

*c*) Counting : the nickel metal disc was directly counted.

The *Co*-58 (71 days half-life) activity was determined by counting the 0.81 *MeV* gamma photopeak (1 $\gamma$/dis.) two days after the irradiation end to allow complete decay of *Co*-58 m (9 hours half-life).

### 3.7 — Al - 27(n,p) Mg - 27

*a*) Target : high purity aluminum metal disc (about 100 mg) in aluminum cans.
Irradiation time : several minutes.

*b*) Chemical : after the irradiation no chemical treatment was carried out on the sample.

*c*) Counting : the aluminum metal disc was directly counted. The *Mg*-27 (9.5 min. half-life) activity was determined by counting 0.83 and 1.01 *MeV* gamma photopeaks as soon as possible after the irradiation.

The decay scheme of *Mg*-27 is not well known. Therefore the *Mg*-27 activity was evaluated assuming the sum of the percent of the 0.83 and 1.01 *MeV* gamma photopeaks equal to 100 and utilizing the photopeaks efficiencies obtained from the calibration curves of the crystal. The Compton distribution of the 1.01 *MeV* gamma was subtracted from the 0.83 *MeV* gamma photopeak. The experimental percent obtained for the two gamma photopeaks are 75 % - (0.83 *MeV*) and 25 % (1.01 *MeV*).

### 3.8 — Fe - 56(n,p) Mn - 56

*a*) Target : high purity iron metal discs (about 100 mg) in aluminum cans.
Irradiation time : several hours.

*b*) Chemical : after the irradiation no chemical treatment was carried out on the sample.

*c*) Counting : the iron metal disc was directly counted.
The *Mn*-56 (2.6 hours half-life) activity was determined by counting 0.84 *MeV* gamma photopeak. The scintillation detector was previously standardized with *Mn*-56 calibrated sources.

### 3.9 — Al - 27(n,$\alpha$) Na - 24

*a*) Target : high purity aluminum metal discs (about 100 mg) in aluminum cans.
Irradiation time : several hours.

*b*) Chemical : after the irradiation no chemical treatment was carried out on the sample.

*c*) Counting : the aluminum metal disc was directly counted. The *Na*-24 (15 hours half-life) activity was determined by counting 1.37 *MeV* gamma photopeak (1 $\gamma$/dis.).
*Na*-24 activity from ($n$,$\gamma$) reaction was found to be very small.

Table IV shows the experimental $A_i$ values obtained in the Ispra 1 and Avogadro *RS* 1 reactors.

# 4 — EXPERIMENTAL RESULTS INTERPRETATION

## 4.1 — Introduction

The experimental data obtained by threshold detector measurements may be expressed in the form of activation rates :

$$A_i = \int_o^\infty \varphi(E)\,\sigma_i(E)\,dE = \int_{E_i}^\infty \varphi(E)\,\sigma_i(E)\,dE \qquad (2)$$

They indicate the reaction probability per second for one nucleus of *i-th* isotope in the differential neutron flux $\varphi(E)$.

If $n$ threshold detectors are used, there are $n$ integral equations of the above type (2), whose solution should be univocally determined. If $n$ is a finite number, univocal determination of $\varphi(E)$ is impossible : to reach a solution a hypothesis on the mathematical function has to be stated.

Several methods (13) have been proposed in order to solve the system of equations (2). They can be divided in two groups :

*a*) Mathematical methods : the assumption on $\varphi(E)$ are of purely mathematical type;

*b*) Perturbation methods : the assumption on $\varphi(E)$ are derived from a fission spectrum $\varphi^o(E)$.

## 4.2 — Mathematical methods

Step, Polygonal, Polynomial methods

Three methods, which are rather similar, assume for $\varphi(E)$ the following shape :

1) Step function

2) Polygonal function

3) Polynomial function

The $n$ integral equations ($n$ is the number of the threshold detectors used) are transformed into a system of linear equations with $n$ unknowns.

The coefficients of the linear system are functions of the differential cross sections and (assumption 1 and 2) of $n + 1$ energy values chosen as discontinuity points for $\varphi(E)$, or (assumption 3) of two energy values, bounding the range into which $\varphi(E)$ will be settled. Complete expressions for the coefficients are reported in (13).

The use of the first two methods may lead to surprising results. In fact, being the real shape of a fast neutron spectrum quite different from the proposed one, if the choice of the boundary energy values has not been suitable, it is possible to obtain, in some energy ranges, negative values for the differential neutron flux. The figures 14 and 15 show some results obtained by these methods, changing the set of boundary energies.

A better solution can be obtained using a larger number of detectors; however the system complexity and the probability of an ill conditioning increase.

*TABLE IV*

| | | $Np$-237 $(n, f)$ $A \times 10^{-13}$ | $U$-238 $(n, f)$ $A \times 10^{-14}$ | $Th$-232 $(n, f)$ $A \times 10^{-15}$ | $S$-23 $(n, p)$ $A \times 10^{-15}$ | $Ni$-58 $(n, p)$ $A \times 10^{-15}$ | $Al$-27 $(n, p)$ $A \times 10^{-16}$ | $Fe$-56 $(n, p)$ $A \times 10^{-17}$ | $Al$-27 $(n, \alpha)$ $A \times 10^{-17}$ |
|---|---|---|---|---|---|---|---|---|---|
| Ispra 1 | | | | | | | | | |
| 3.7 *MW* | *PH* 3 | 4.17 | 3.39 | 9.21 | 4.07 | 6.15 | 2.54 | 7.63 | 5.28 |
| | 4 *DH* 1/1 | | | | 6.57 | 11.17 | | | 9.71 |
| | 4 *DH* 1/2 | | | | 4.61 | 7.79 | | | 6.91 |
| | 4 *DH* 1/3 | | | | 3.27 | 5.30 | | | 4.94 |
| | 4 *DH* 1/4 | | | | 2.15 | 3.59 | | | 3.35 |
| | 4 *DH* 1/5 | | | | 1.42 | 2.30 | | | 2.20 |
| | 4 *DH* 1/6 | | | | 0.869 | 1.57 | | | 1.55 |
| | 4 *DH* 1/7 | | | | 0.588 | 1.02 | | | 1.06 |
| | 4 *DH* 1/8 | | | | 0.395 | 0.705 | | | 0.751 |
| 5 *MW* | 4 *DH* 1/1 | | | | | 15.3 | | | 12.5 |
| Avogadro *RS* 1 - pos. *D*3 | | | | | | | | | |
| 1.8 *MW* | 1 | 246 | 452 | | 795 | 1200 | | | 811 |
| | 2 | | | | 798 | 1180 | | | 803 |
| | 3 | 320 | 520 | | 851 | 1340 | | | 913 |
| | 4 | | | | 990 | 1450 | | | 977 |
| | 5 | 249 | 430 | | 726 | | | | 750 |
| | 6 | 258 | 451 | 1270 | 744 | 1080 | | | 731 |
| | 7 | 142 | 252 | 645 | 449 | 697 | | | 468 |
| | 8 | | | | 490 | 775 | | | 502 |
| | 9 | 156 | 252 | 608 | | | | | |

The polynomial method assumption is that the solution be of the following type :

$$\varphi(E) = a_o + a_1 E + \ldots\ldots + a_{n-1} E^{n-1}$$

It is easy to see that this assumption leads to an ill conditioned linear system; in fact the coefficient of the *k-th* unknown in the equation of *i-th* detector is :

$$C_{ik} = \int_{E_1}^{E_{n+1}} E^{k-1} \sigma_i(E)\ dE$$

It follows that, with increasing $k$, the values of $C_{ik}$ exponentially increase. The hyperplanes that represent such a type of system are nearly parallel.

By applying this method to our experimental data, we never obtained satisfactory results : using 6, 7 or 8 detectors, we never noticed a cosine of the angle between the hyperplanes smaller than 0.9999.

A typical result obtained by this method is shown in fig. 14.

All the calculations relative to the above explained methods have been carried out by a 7090 IBM digital computer.

Dierckx method

Theoretical considerations and the analysis of neutron spectra obtained by nuclear emulsions enable to assume the fast neutron spectrum as a sequence of exponential functions. This observation, together with a hypothesis on the cross-section's shape, allowed Dierckx (14) to elaborate a method that gives satisfactory results. A result obtained applying this method is shown in fig. 15.

It has to be pointed out that the request of linearised cross-sections is a limit for the method itself; in fact, in our calculations, in the first energy band the result is not correct (the exponential value is too high) because the detector used ($U$-238 )presents, in that band, a $\sigma(E)$ having a shape very far from a straight line.

In order to avoid the heavy calculations required and to suppress the limiting condition on $\sigma(E)$, a modification of the Dierckx's method to be used in connection with a digital computer is possible.

### 4.3 — Perturbation methods

A certain number of methods use the fundamental hypothesis that the unknwon shape $\varphi(E)$ is a deformation of a fission spectrum $\varphi^o(E)$ : the determination of the perturbation function F defined by the expression (3) is, therefore, the new problem.

$$\varphi(E) = F.\ \varphi^o(E) \tag{3}$$

Uthe (15) proposed for $F$ a polynomial form :

$$F = a_o + a_1 E + \ldots\ldots\ldots + a_{n-1} E^{n-1} \tag{4}$$

The difficulties we meet in using this method are just the same we met in the mathematical method called "polynomial".

A second type of perturbation function is suggested by O.W. Dietrich (16). $\varphi(E)$ is calculated by a removal theory, used in the sense that a neutron having once collided is lost for the fast spectrum. Following this development line, $F$ results :

$$\frac{1}{1 + \alpha . E^{-0.725}} \tag{5}$$

where the $\alpha$ value is calculated from the experimental data.

We have not used this method because the above removal theory is not correct for $E < 2\ MeV$.

J. Grundl and A. Usner (17), from the Cranberg (18) and Leachman (19) form of $\varphi^0(E) = k \cdot e^{-0.775E} \sqrt{E}$, proposed for the fast neutron flux the form

$$\varphi(E) = k \cdot \sqrt{E} \cdot e^{-\beta E} \tag{6}$$

The $\beta$ parameter accounts for the spectrum deformation.

This method has been used for the analysis of the experimental data reported in table IV. The analysis of the *PH* 3 position data shows that the method can be usefully applied with detectors of threshold energy higher than 2 *MeV*. In fact, large discrepancies in the $\beta$ values have been found with detectors of lower energy. This limitation is substained also by the experimental data obtained in the Avogadro *RS* 1.

### 4.4 — Iterative method

Among the different methods of "perturbation" type the following iterative method may be included. First of all $E^*_{eff}$ and $\sigma^*_{eff}$ have to be defined for all the $n$ threshold detectors; the asterisk means that the spectrum used to obtain the effective energies and cross sections is a fission one. The values we have used are reported in table I.

In a zero order approximation we may write :

$$A_i = \int_0^\infty \varphi^o(E)\, \sigma_i(E)\, dE = \sigma^*_{eff\,i} \int_{E^*_{eff\,i}}^{E_{n+1}} \varphi^o(E)\, dE = \sigma^*_{eff\,i} \cdot \Phi^1(E^*_{eff\,i})$$

It follows :

$$\Phi^1(E^*_{eff\,i}) = \frac{A_i}{\sigma^*_{eff\,i}} \tag{7}$$

In the present calculation the value of $E_{n+1}$ has been fixed as 12 *MeV*. In fact using the Watt formula :

$$\Phi^o(12\,MeV) \sim 2 \cdot 10^{-4} \cdot \Phi^o(0\,MeV)$$

The values of $E^*_{eff1}, E^*_{eff2}, \ldots\ldots\ldots, E^*_{eff(n-1)}, E_{(n+1)}$ divide the energy axis into $n$-1 intervals. In order to solve the problem we assume $\varphi(E)$ to be a continuous function that in $i$-*th* interval may be described by the expression :

$$\varphi(E) = \varphi_{i+1} \cdot e^{\frac{-h}{i}(E - E_{eff(i+1)})}$$

where $\varphi_{i+1}$ is the value assumed by $\varphi(E)$ in the inferior limit of $(i+1)$-*th* interval; in the last interval the shape of $\varphi(E)$ is assumed to be :

$$\varphi(E) = k \cdot e^{\frac{-h}{n-1} \cdot E}$$

For this last interval we can write the system :

$$\Phi^1\ (E^*_{eff\ n}) = \int_{E^*_{eff\ n}}^{E_{n+1}} k \,.\, e^{-h_{(n-1)}E}\, dE \tag{8}$$

$$\Phi^1\ (E^*_{eff\ (n-1)}) = \int_{E^*_{eff\ (n-1)}}^{E_{n+1}} k \,.\, e^{-h_{n-1}E}\, dE$$

The solution of (8) gives the values of $k$ and $h_{n-1}$, and then the first order approximation $\varphi^1(E)$ between $E^*_{eff(n-1)}$ and $E_{n+1}$.

Now for the $\varphi^1(E)$ complete determination it is possible to use an iterative method. Infact, from the knowledge of $\varphi^1{}_{t+1}$ we may write :

$$\Phi^1\ (E^*_{eff\ t}) = \Phi^1\ (E^*_{eff\ (t+1)}) + \int_{E^*_{eff\ t}}^{E^*_{eff\ (t+1)}} \varphi^1{}_{t+1} \,.\, e^{-h_t (E - E_{eff\ (t+1)})}\, dE \tag{9}$$

The solution of the equation (9) gives $h_t$ and then $\varphi^1{}_t$.

In this manner in the range $E^*_{eff\ 1} - E_{n+1}$ a first order approximated value $\varphi^1\ (E)$ is defined. An extrapolation to energy lower than $E^*_{eff\ 1}$ is mathematical possible. - By $\varphi^1$ and $\sigma_t\ (E)$, the values $E^1{}_t$ of the effective energy in $\varphi^1(E)$ spectrum, relative to $\sigma^*_{eff}$, are calculated. Now is possible to evaluate a new approximation $\varphi^2(E)$ by operating in the way above reported, where naturally, the $E^*_{eff\ t}$ are replaced by $E^1{}_t$. The method is cyclic. (fig. 16, 17).

For every cycle we can calculate the values :

$$A^k{}_t = \int_{E_t}^{E_{n+1}} \varphi^k\ (E) \,.\, \sigma_t\ (E)\ dE$$

The comparison between $A^k{}_t$ and $A_t$ gives the reliability of $\varphi(E)$.

The fig. 18 shows this comparison for 9 iteration cycles. It has to be remarked that, for $\varphi^9(E)$, the deviation from $A_t$ experimental values are lower than 1 %.

## 5 — ACKNOWLEDGEMENTS

The authors wish to thank Prof. G. Bertolini and Dr. G. Cecchini for helpful suggestions and discussions, Dr. R. Fantechi for standard sources, Dr. G. Restelli and F. Cappellani for some alpha-spectroscopy measurements, Dr. Guerri and co-workers for the kind co-operation in using IBM 7090 digital computer.

The kindness of SORIN and CNEN made possible the irradiations in the Avogadro *RS* 1 and Ispra 1 reactors and the publication of figures 3, 4 and 5.

## BIBLIOGRAPHY


1 — I. H. HALPERN — Annual Rev. of Nucl. Sci. **9**, 245 (1959).

2 — H. LISKIEN, A. PAULSEN — "Compilation of cross sections for some neutron induced threshold reactions" — Euratom Report EUR 10.e (1962).

3 — R. BEAUGE — "Sections efficaces pour les détecteurs de neutrons par activation recommandées par le groupe de Dosimétrie d'Euratom" — (1963)

4 — G. S. HURST, J. A. HARTER, P. N. AMSLEY, W. A. MILLS, M. SLATER, P. W. REINHARDT — Rev. Sci. Instr. **27**, 153 (1956).

5 — A. BRODSKY, L. W. FAGG — NRL 4746 (1956).

6 — D. BINDER — Rev. Sci. Instr. **31**, 902 (1960).

7 — C. D. CORYELL, N. SUGARMAN — Radiochemical Studies : The fission Products — NNES — McGraw Hill (1951).

8 — G. P. FORD, J. S. GILMORE — LA 1997 (1956).

9 — R. F. COLEMAN, B. E. HAWKER — J. Inorg. and Nucl. Chem. 14, 8-13 (1960).

10 — L. KATCOFF — Nucleonics **18**, No. 11, 201-208 (1960).

11 — A. TURKEVICH, J.B. NIDAY — Phys. Rev. **84**, 52 (1951).

12 — M. BRESESTI, R. LANZ, A. M. DEL TURCO — To be published in "Annali di Chimica".

13 — P. DELATTRE — C.E.A. 1979 (1961).

14 — R. DIERCKX — C.E.N. — R-2128 (1961).

15 — P. H. UTHE — "Attainment of neutron flux spectra from foil activation, Thesis USA-FIT-TR-57-3 (March 1957).

16 — O. W. DIETRICH — "Fast neutron spectra by threshold detector activation", Symposium de la Société Européenne d'Energie Atomique — Risö (1960).

17 — J. GRUNDL, A USNER — Nucl. Sci. and Eng. **8**, 598-607 (1960).

18 — L. CRANBERG — Phys. Rev. **103**, 662-670 (1956).

19 — R. B. LEACHMAN — Conférence de Genève 1955 — P/592.

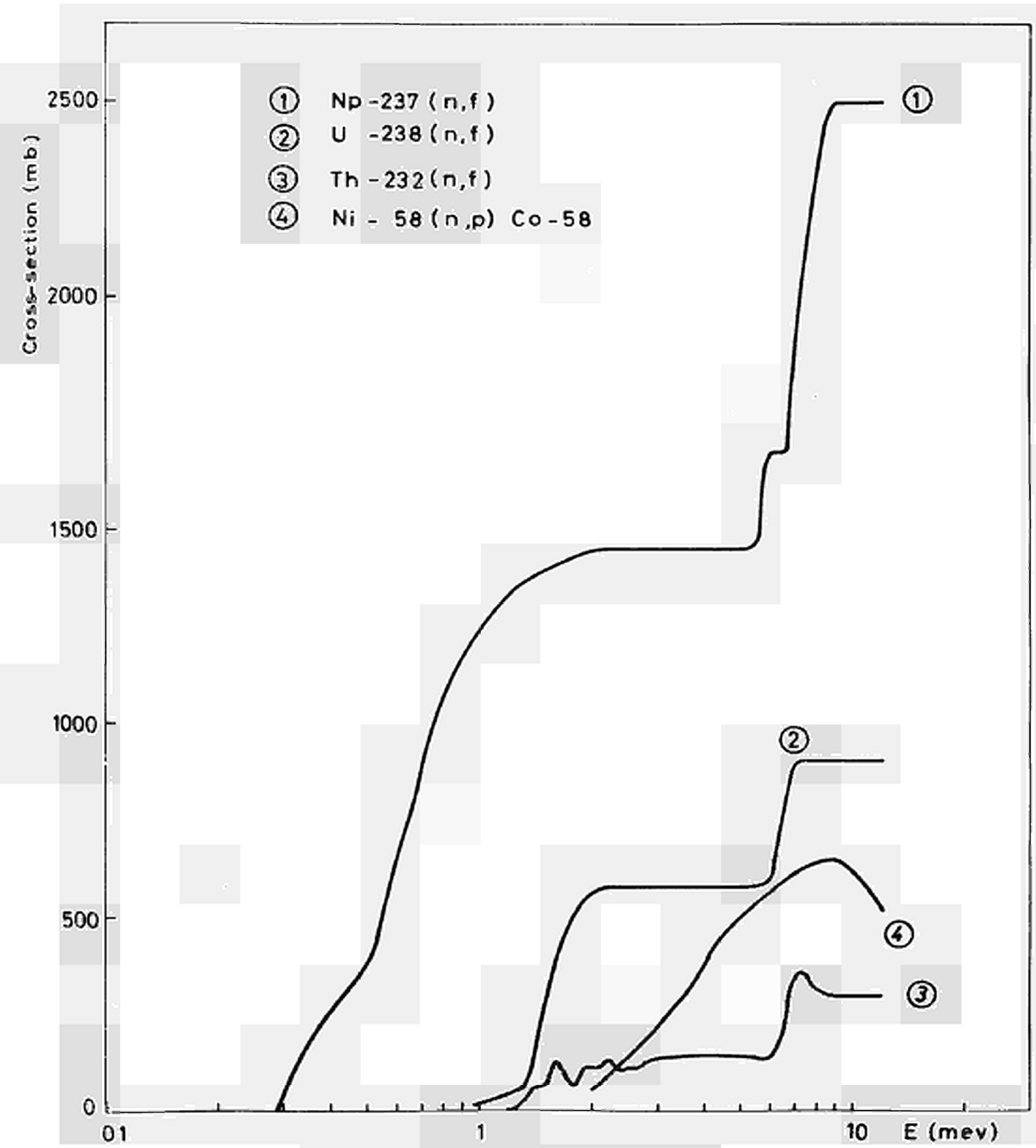


Fig. 1 — Threshold reaction cross-section

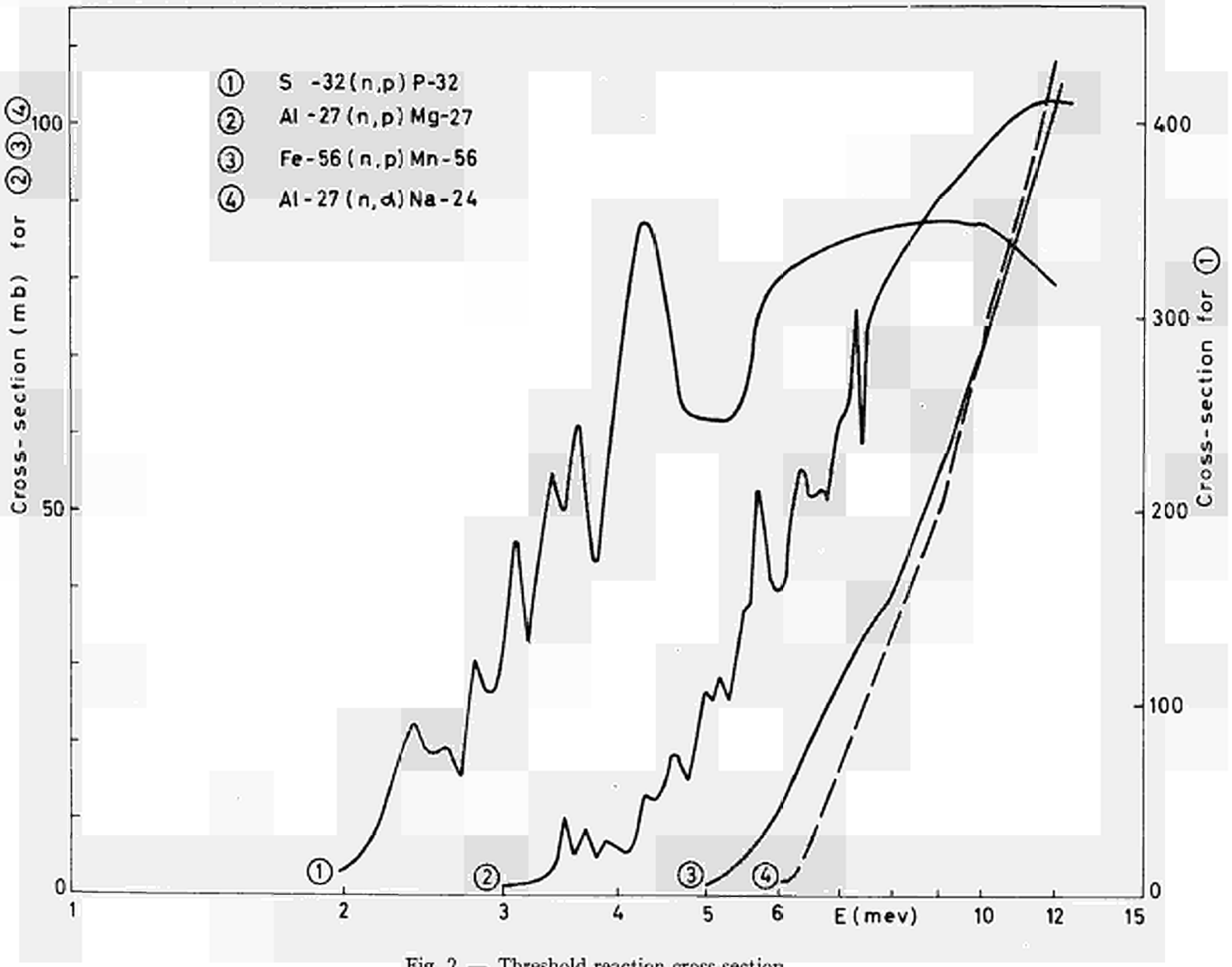


Fig. 2 — Threshold reaction cross-section

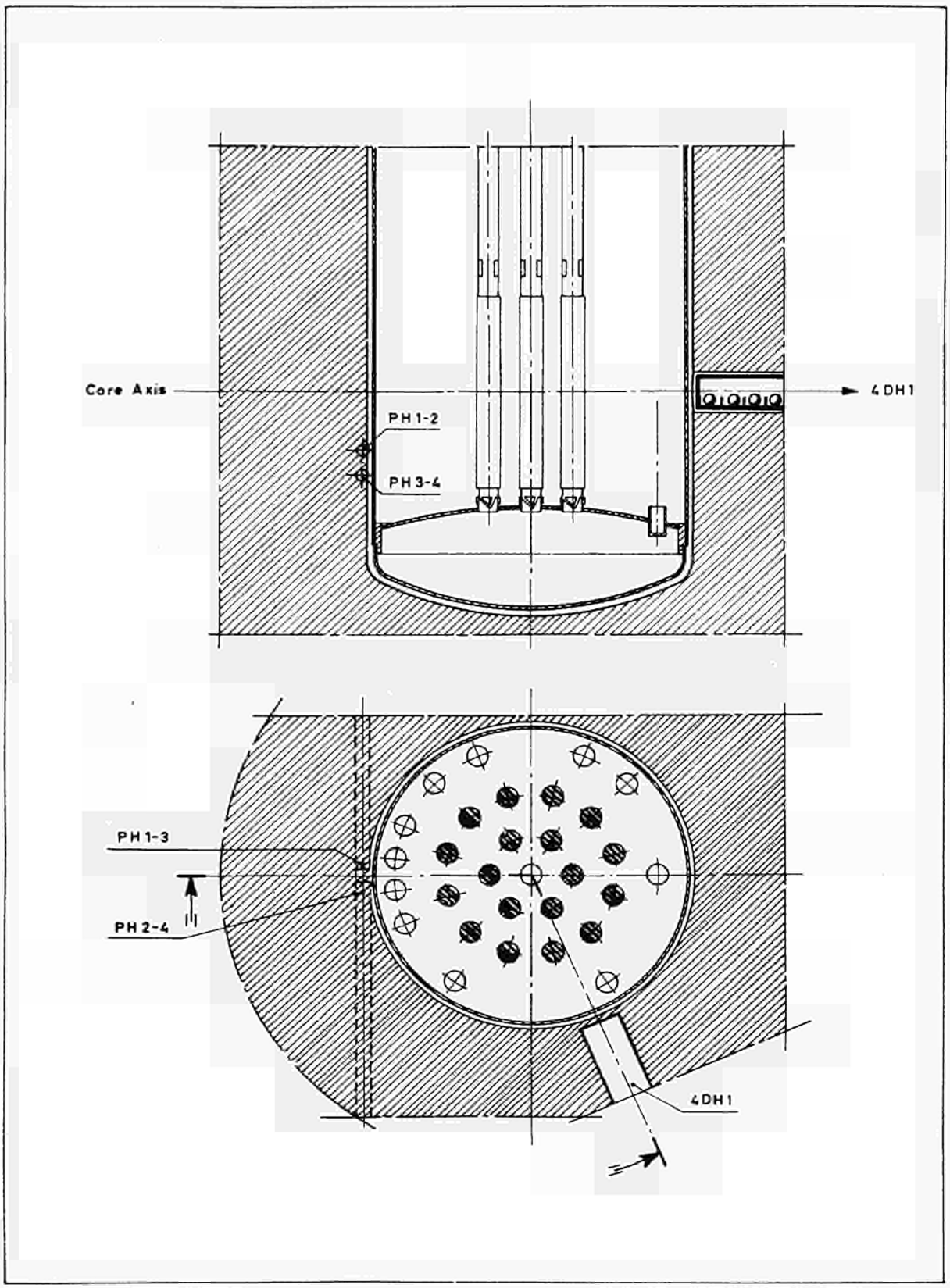


Fig. 3 — Ispra 1 reactor - facilities used in the experiments

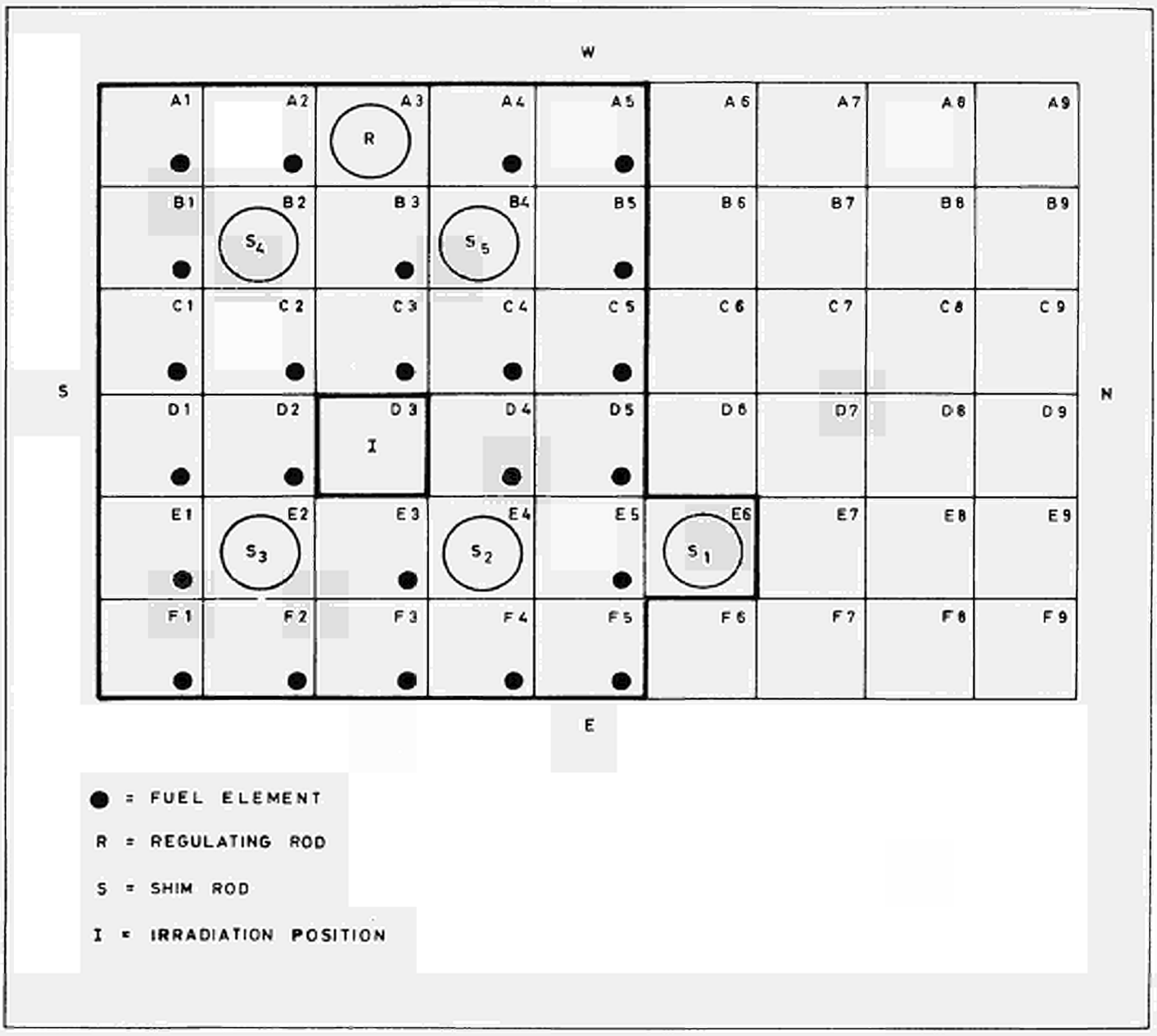


Fig. 4 — Core configuration in the Avogadro RS I reactor

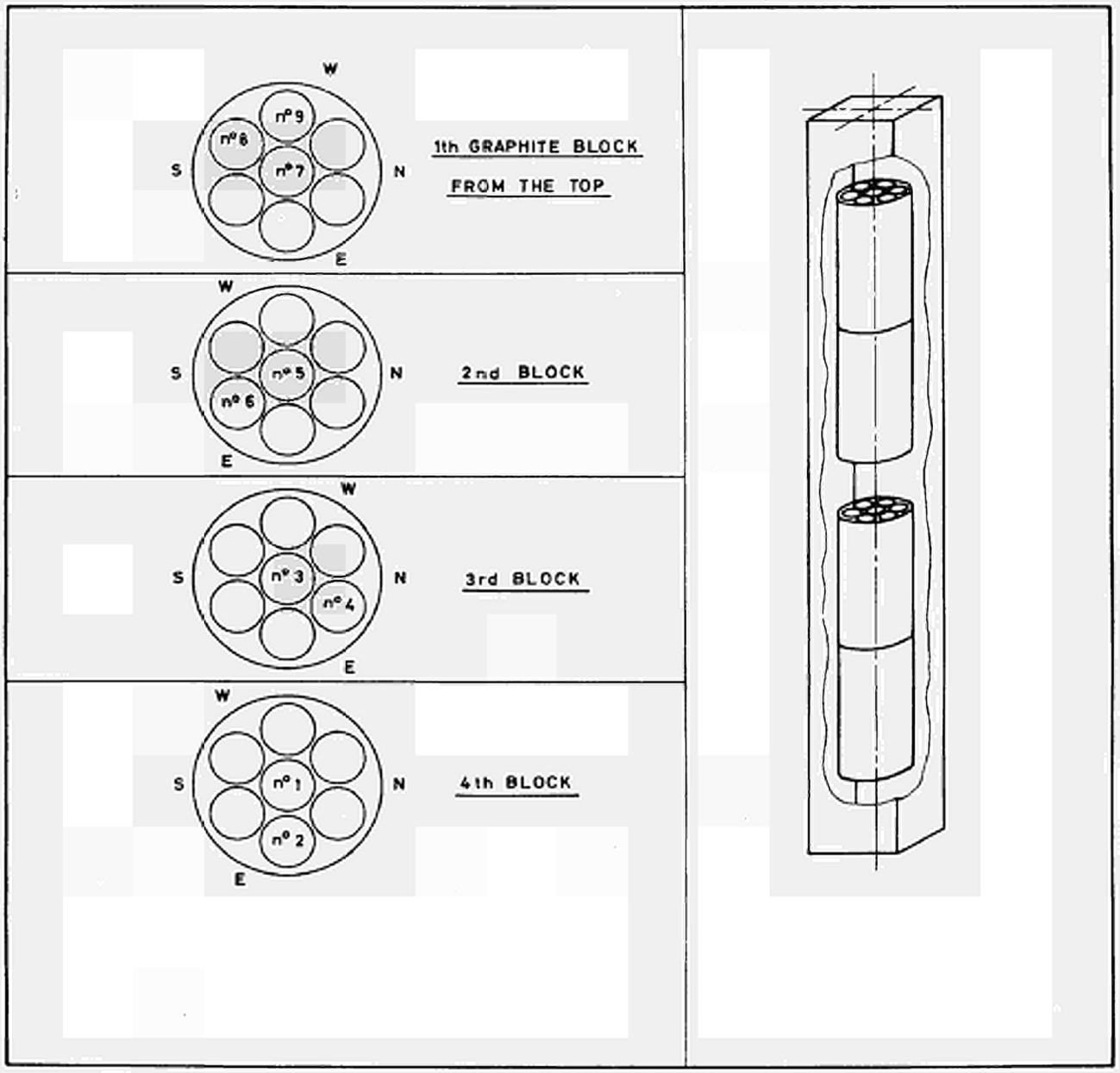


Fig. 5 — Irradiation positions in the Avogadro RS I reactor

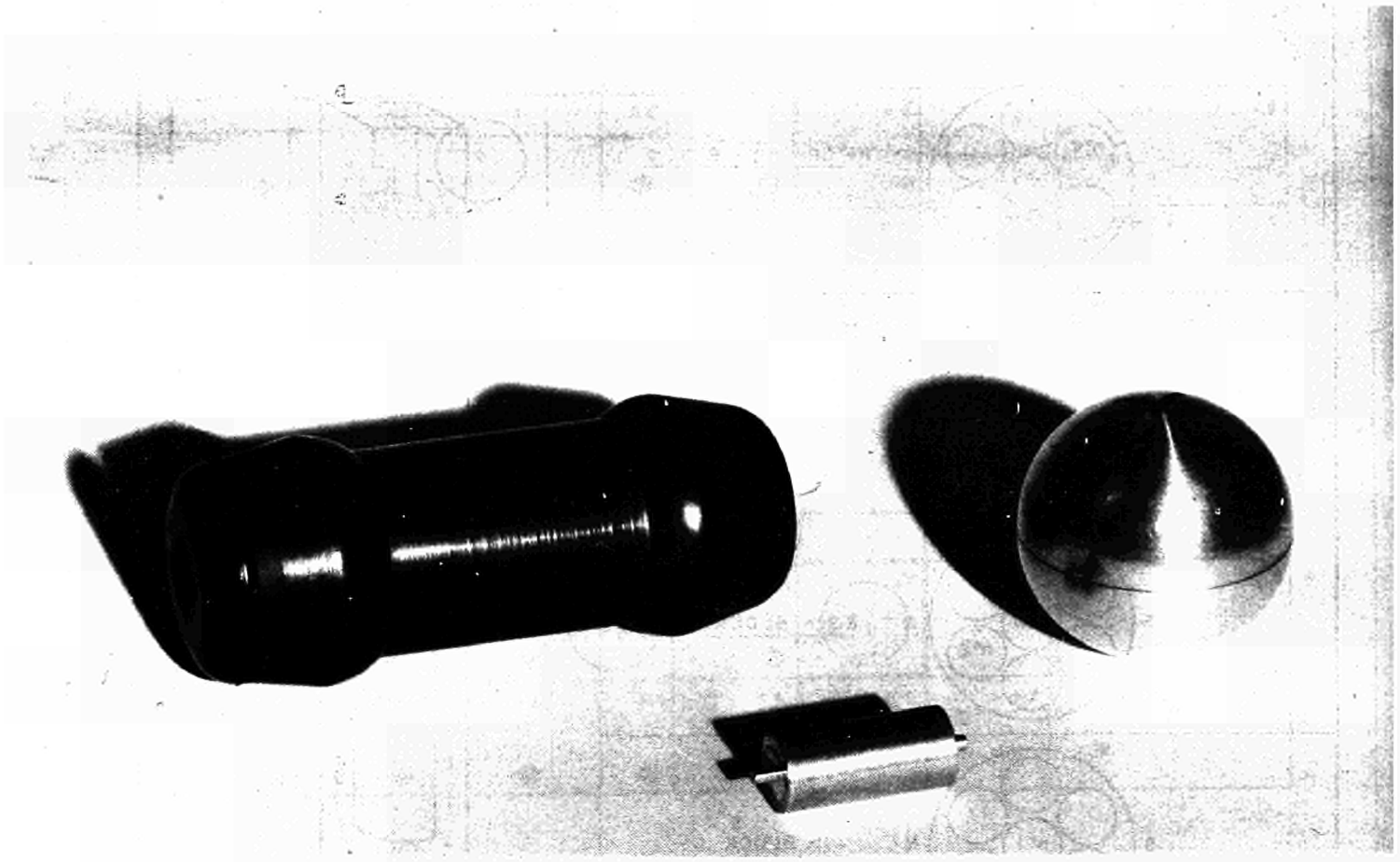

Fig. 6 — Viton, aluminum and cadmium containers

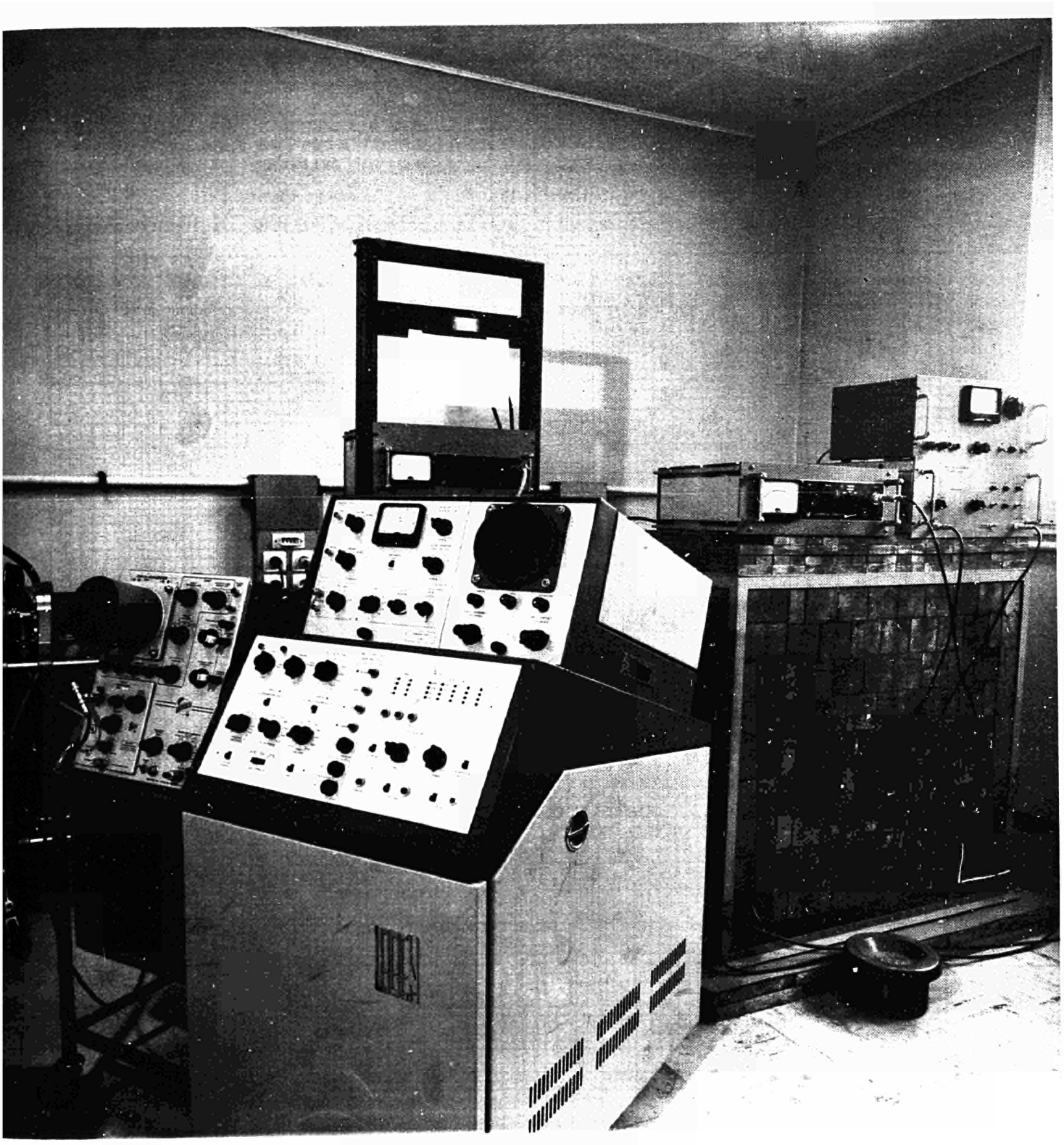

Fig. 7 — Gamma spectrometer

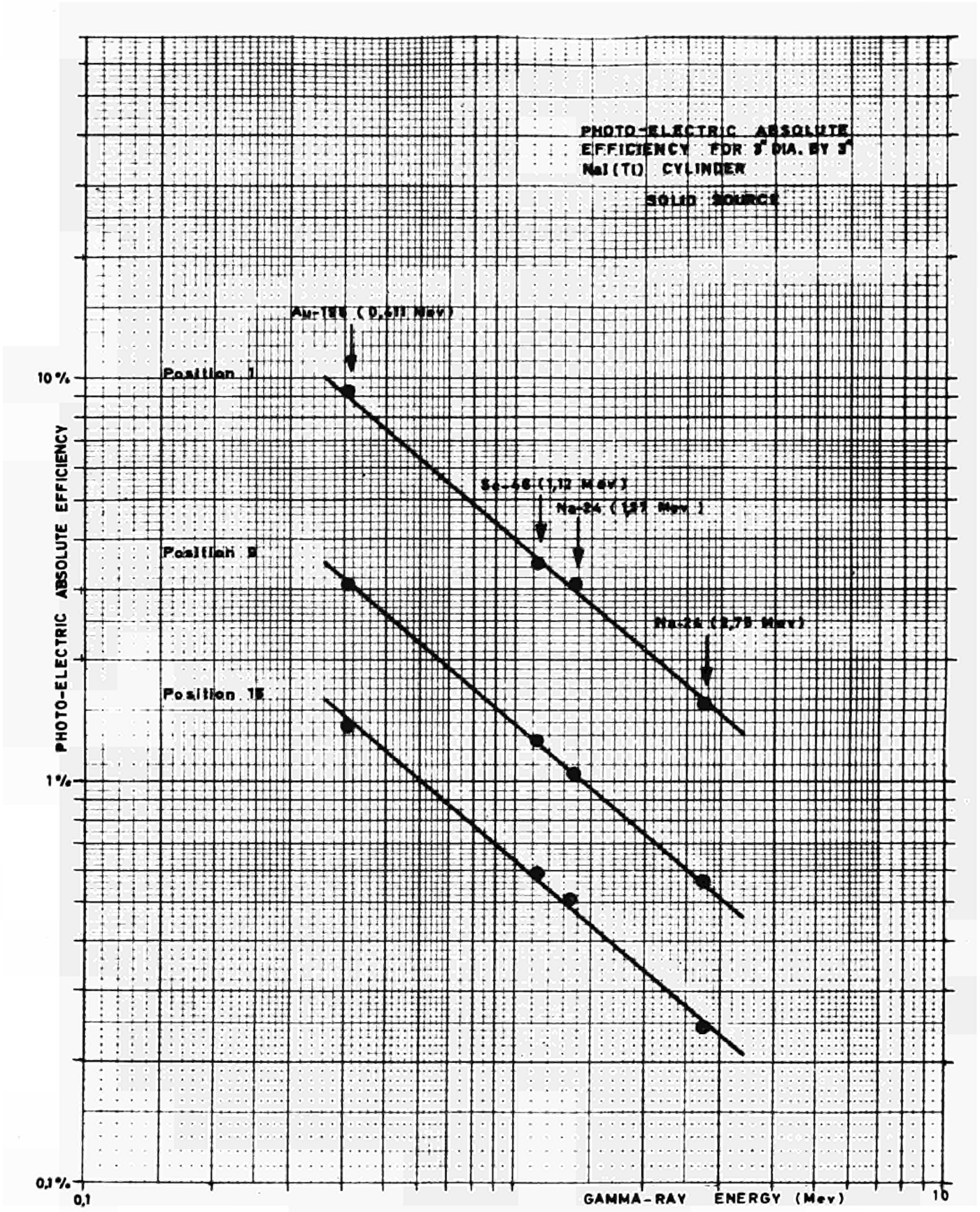


Fig. 8*a*— Efficiency curves for solid sources

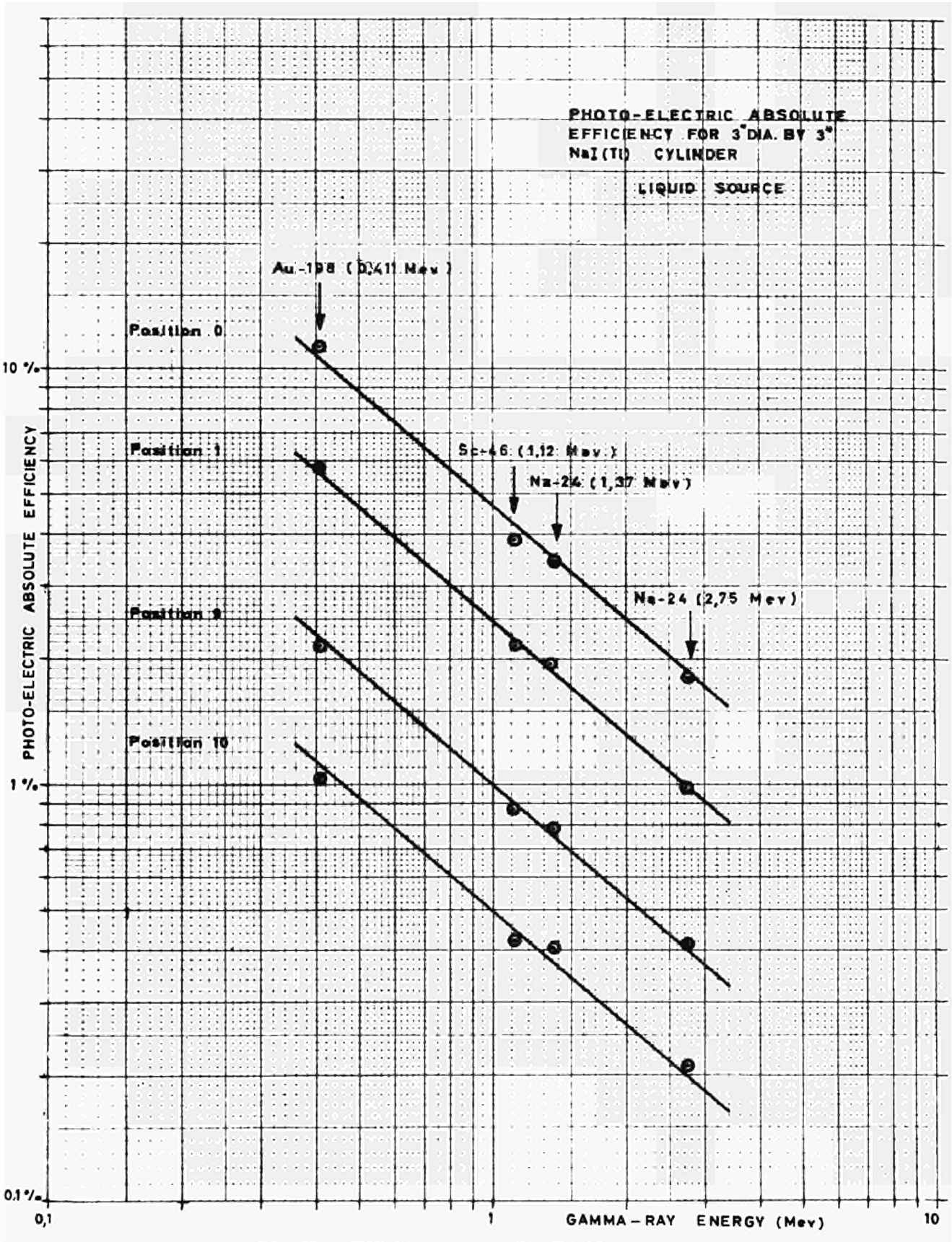


Fig. 8*b*— Efficiency curves for liquid sources

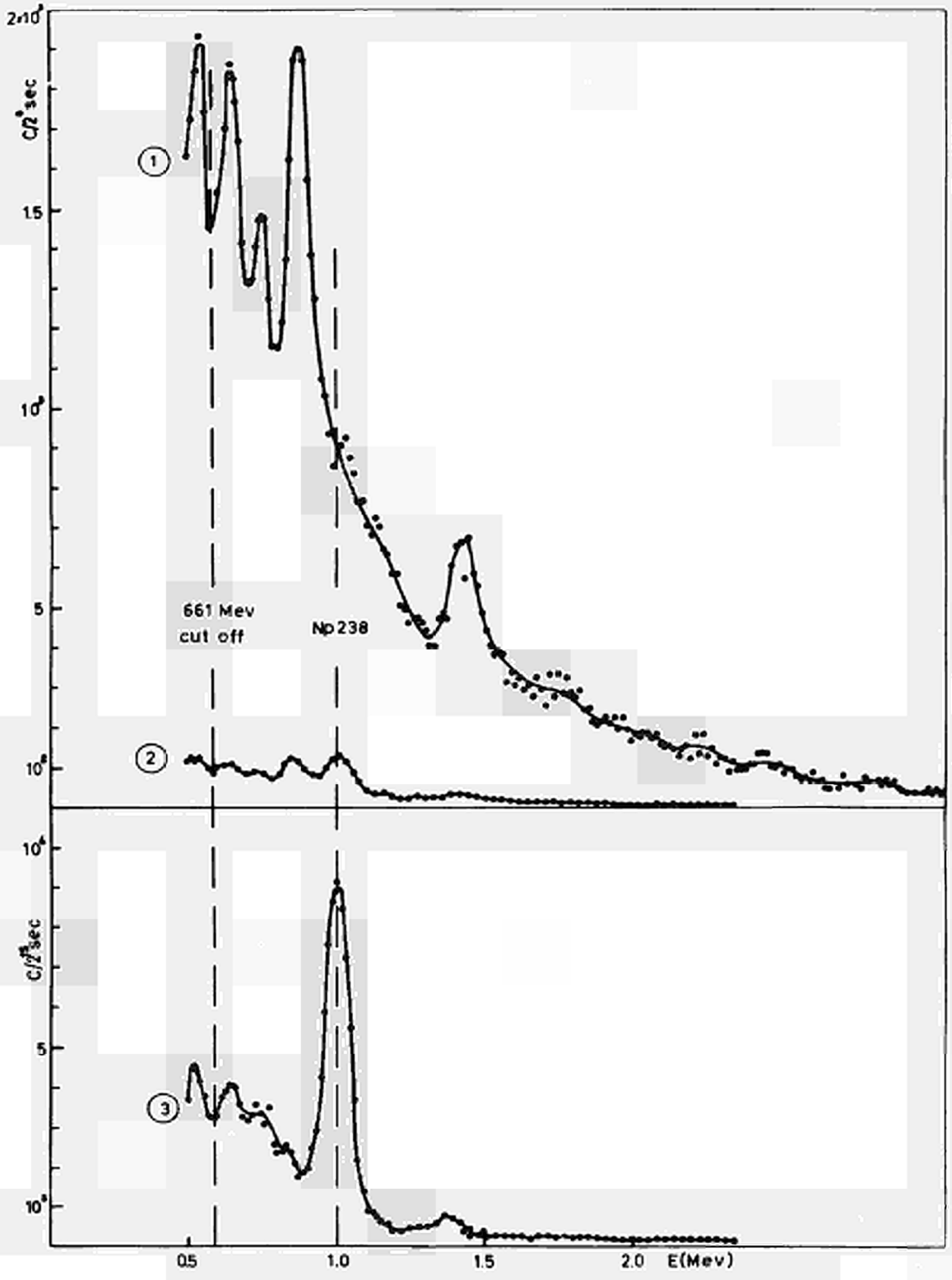


Fig. 9 — Gamma spectra : 1) fission products on catcher;
2) and 3) absorber.

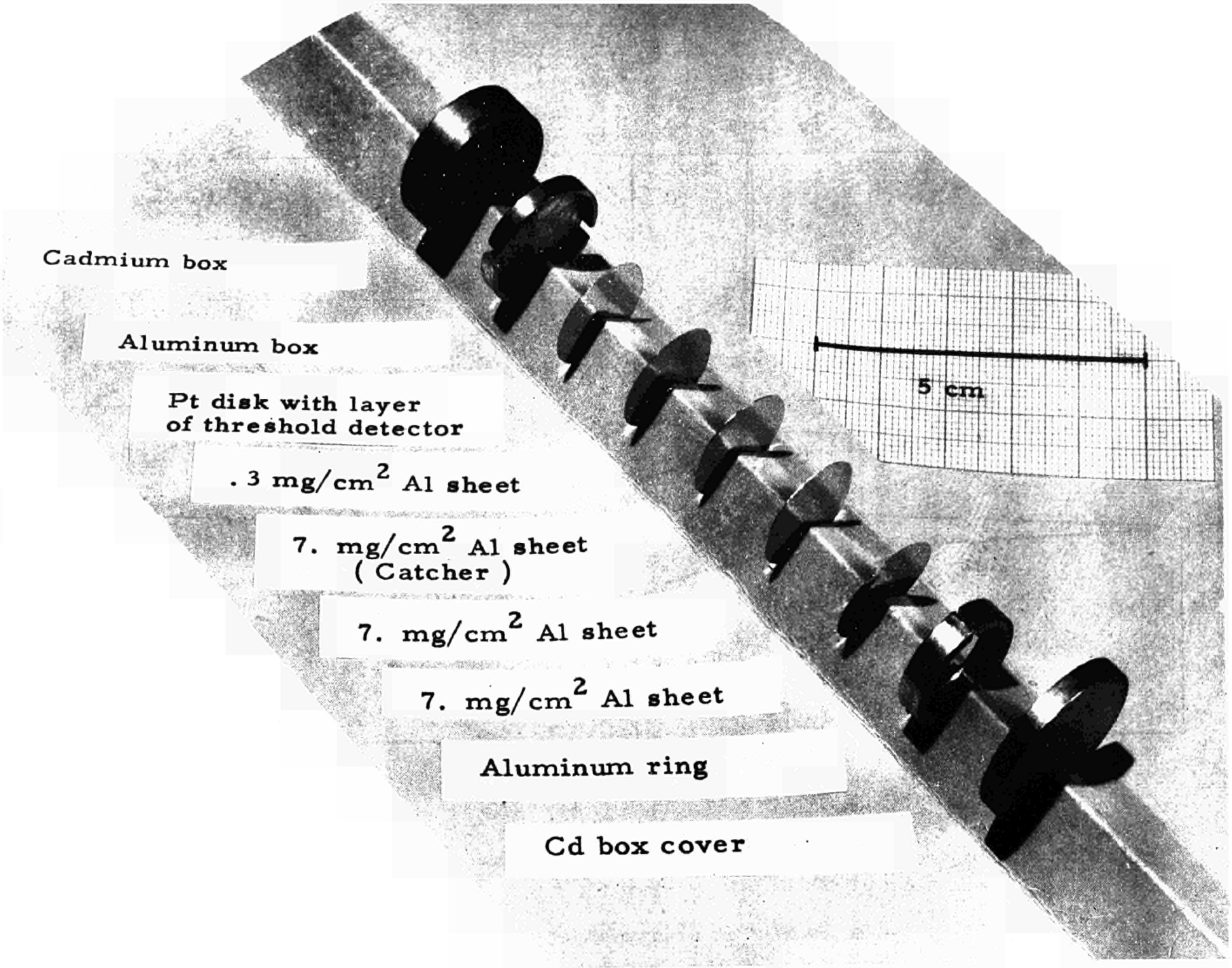


Fig. 10 — Irradiation device used in the catcher method

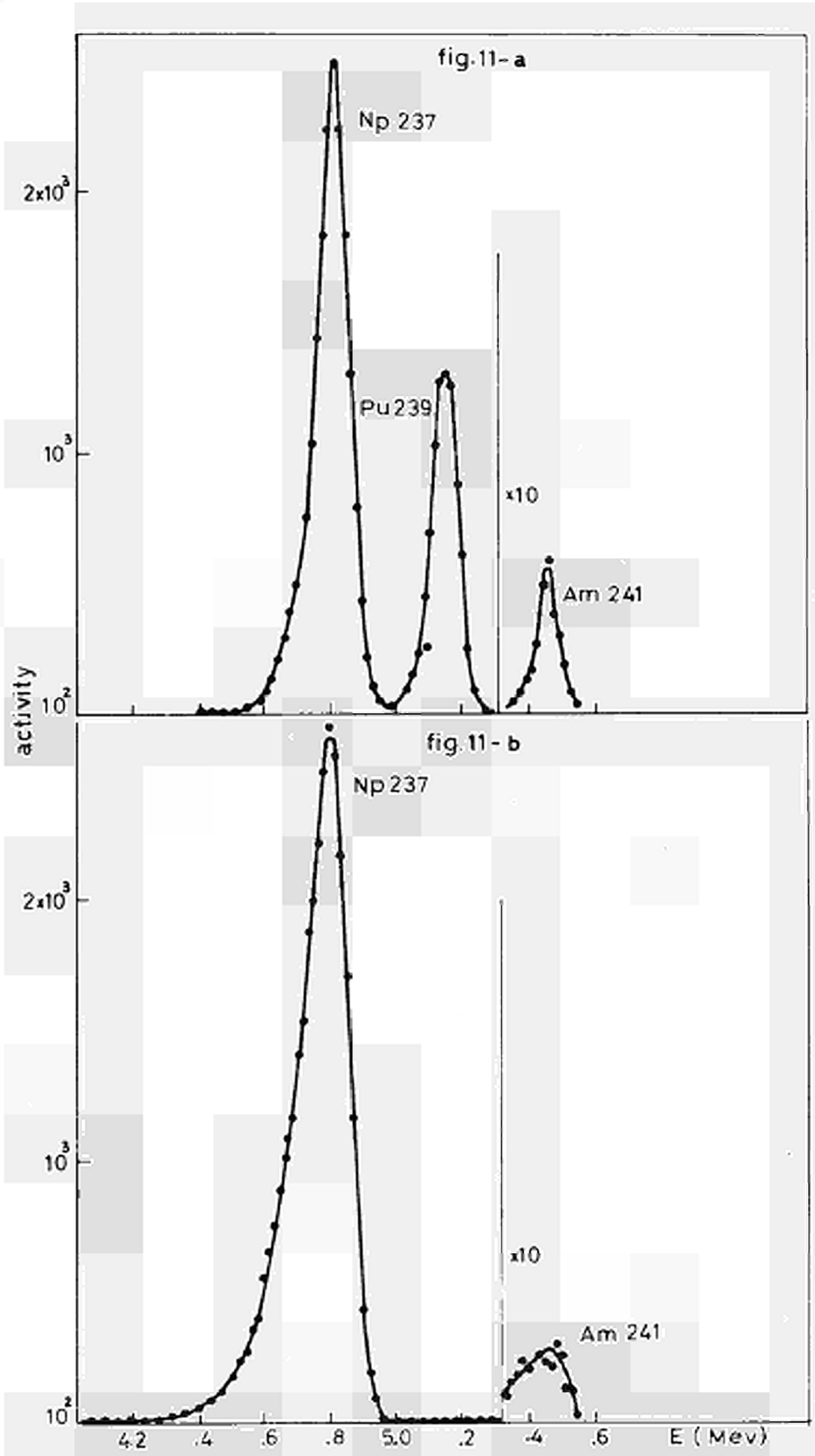


Fig. 11 — Alpha spectrum of the Np-237 solution before (A) and after (B) purification

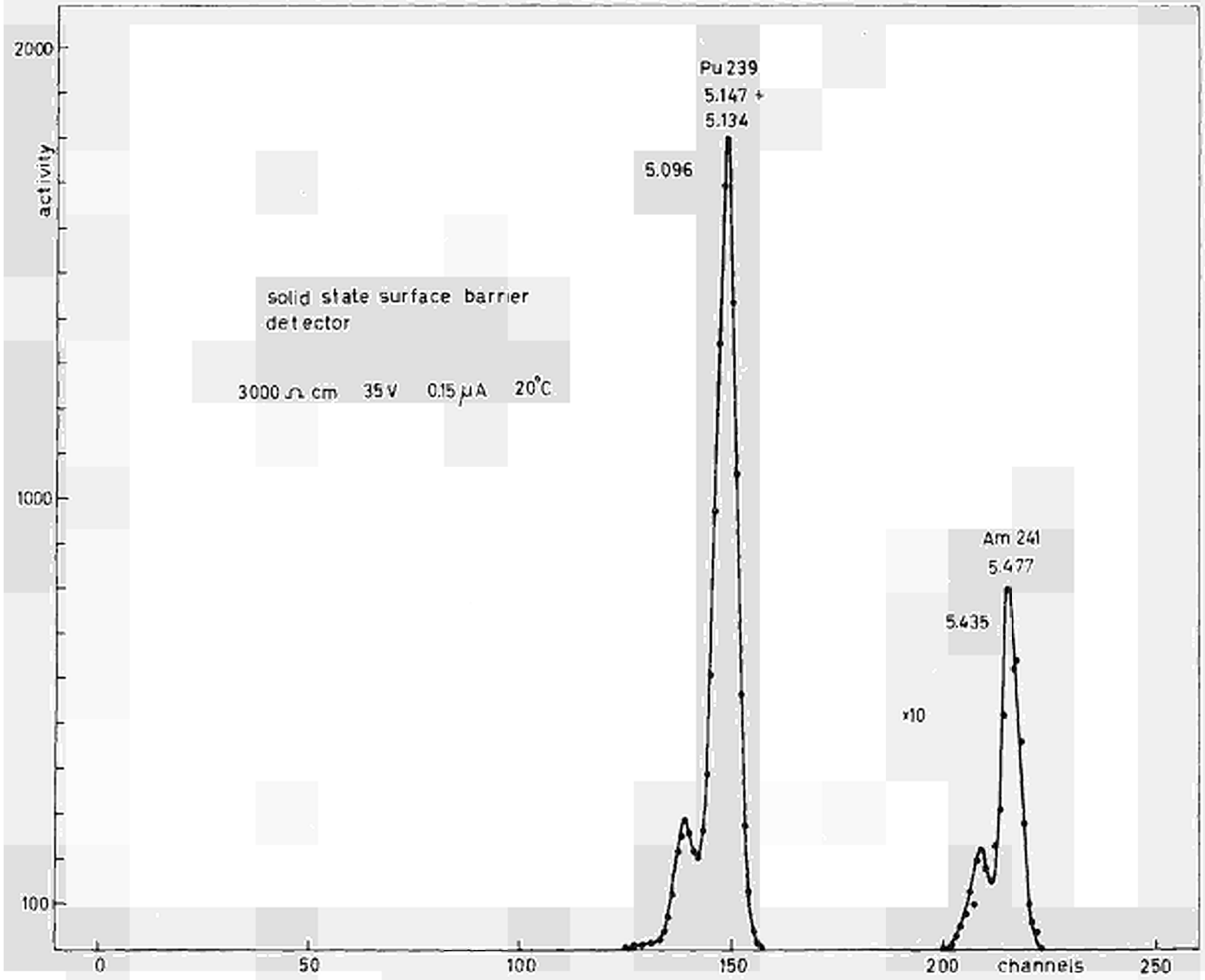


Fig. 12 — Alpha spectrum of the Pu-239 solution.

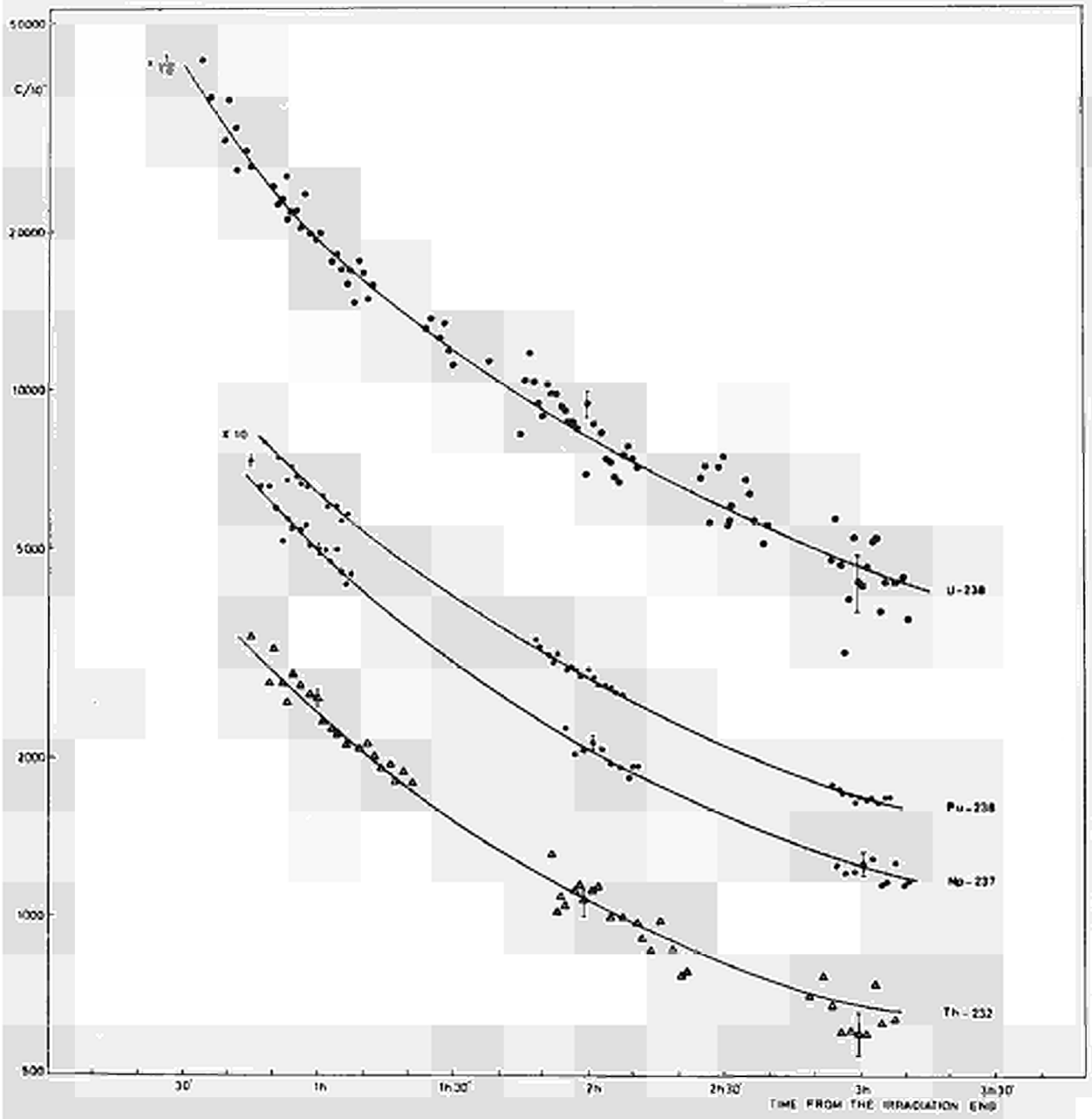


Fig. 13 — Comparison of Np-237, U-238, Th-232, Pu-239 fission products gamma decay

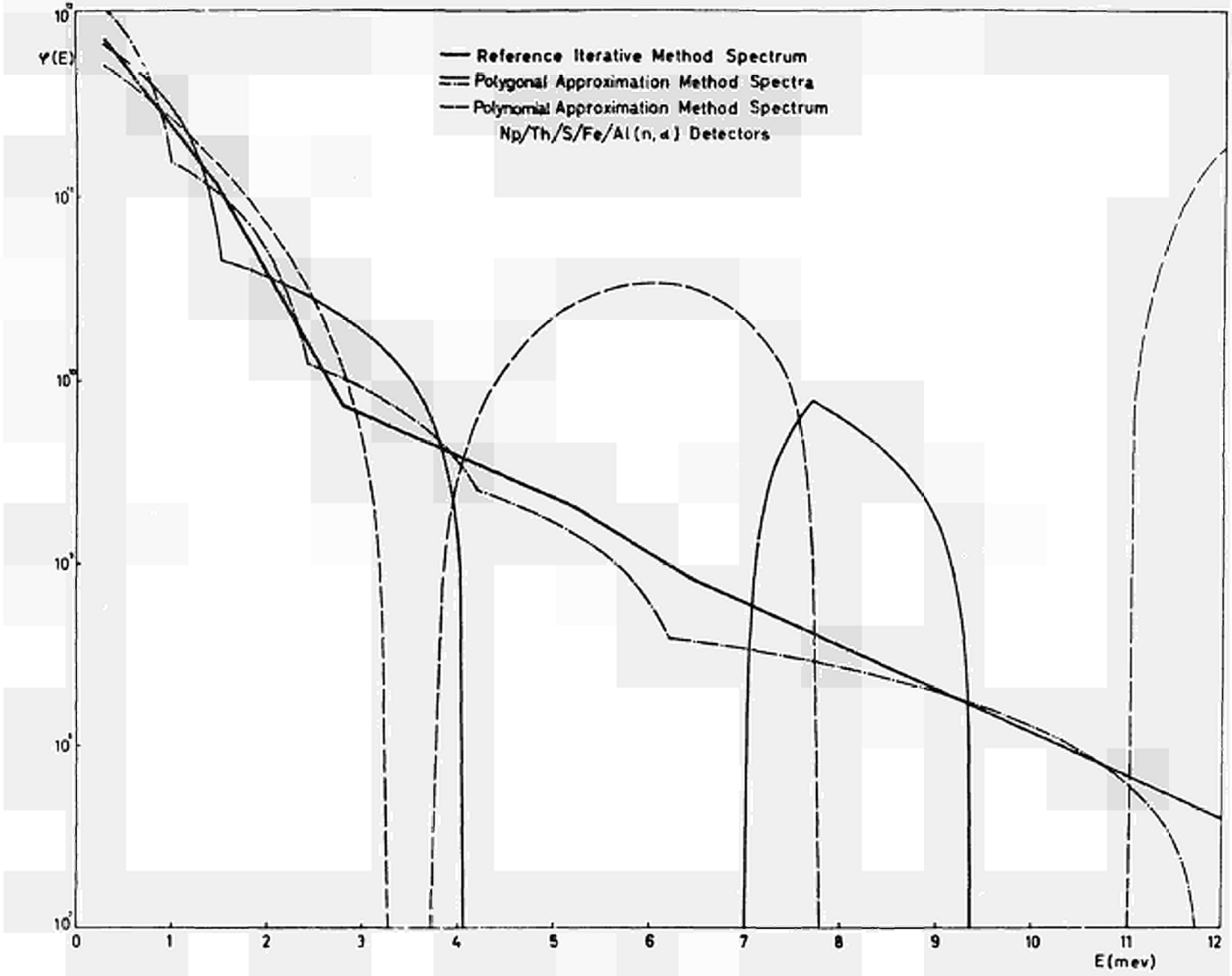


Fig. 14 — Fast neutron spectra

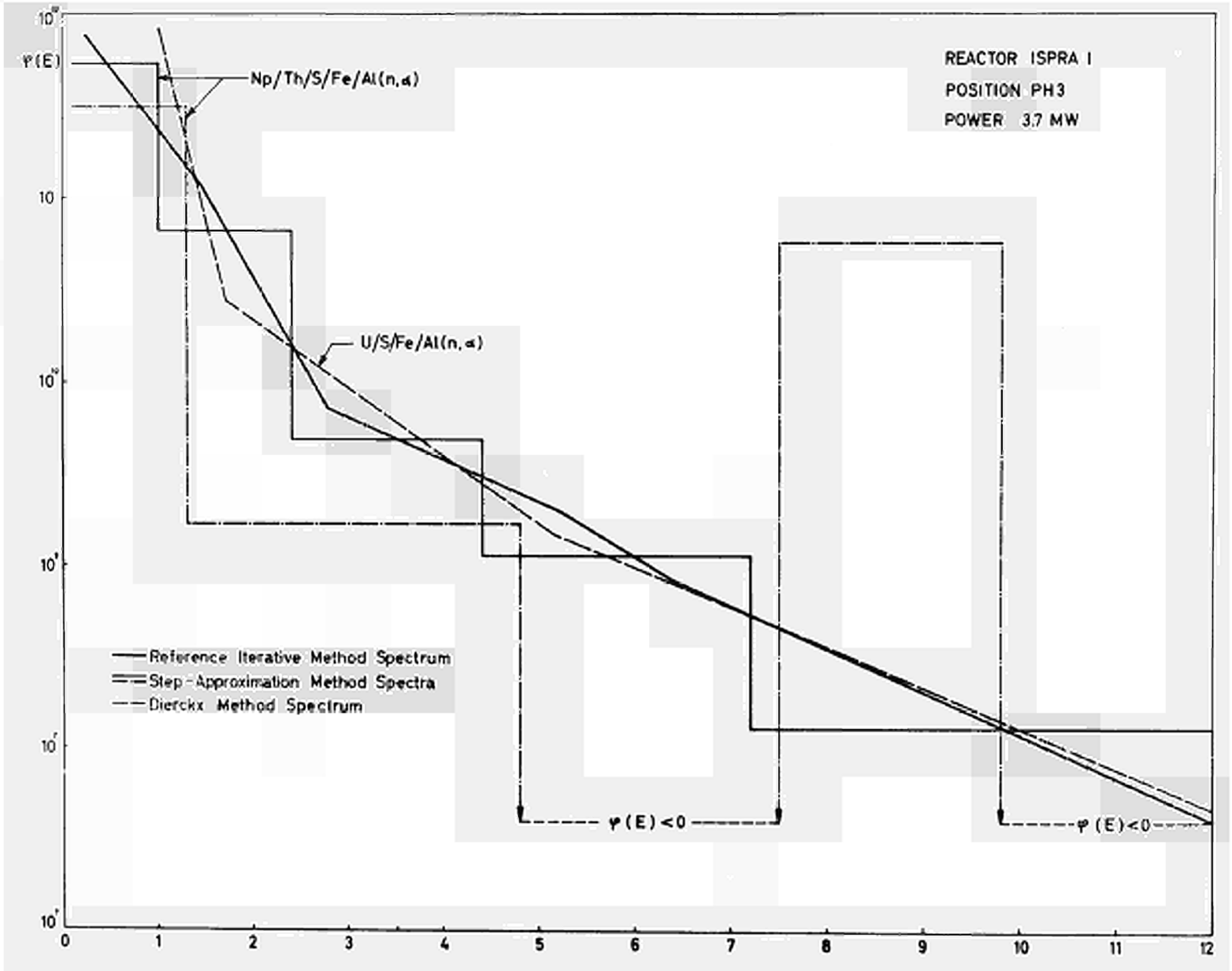


Fig. 15 — Fast neutron spectra

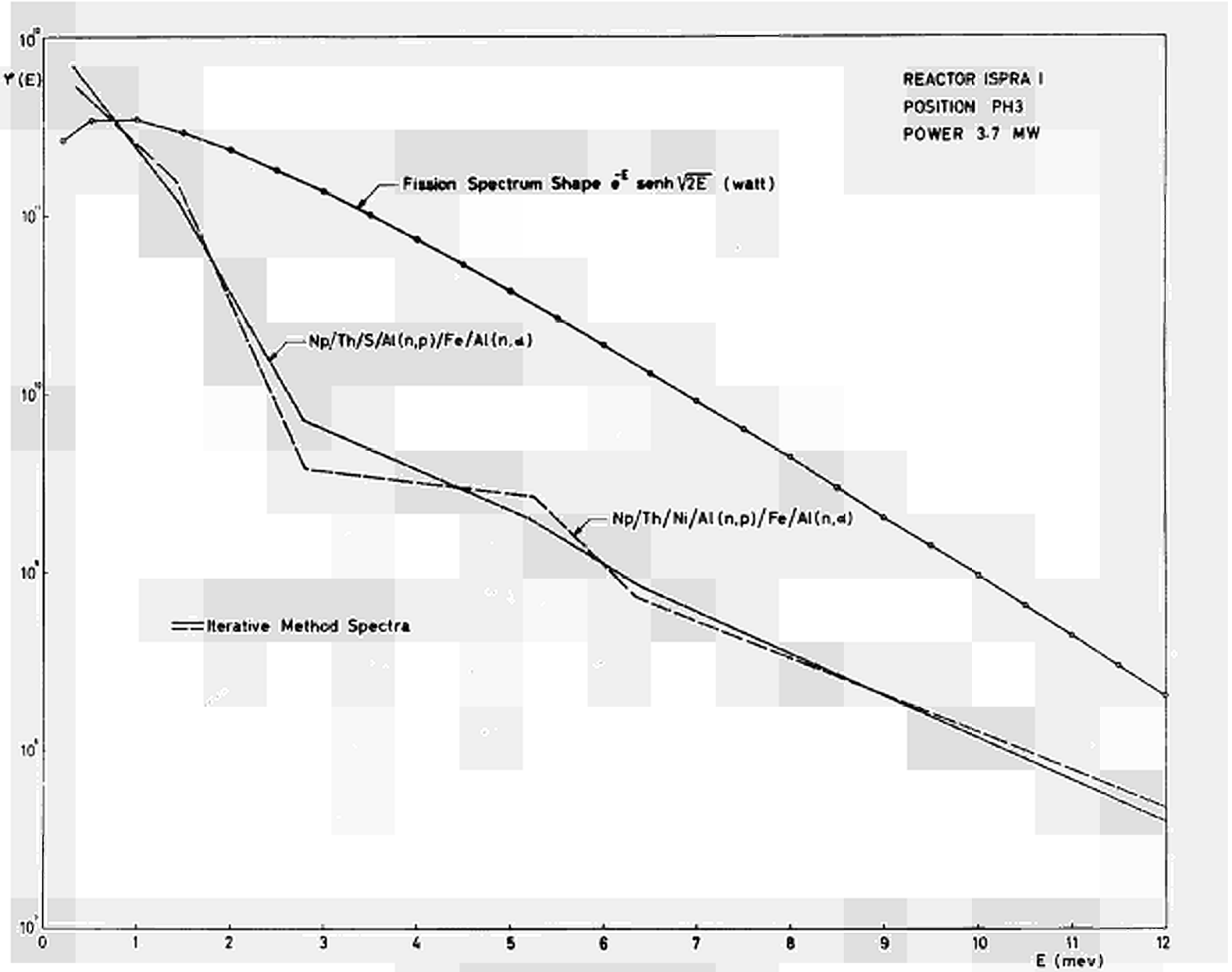


Fig. 16 — Fast neutron spectra

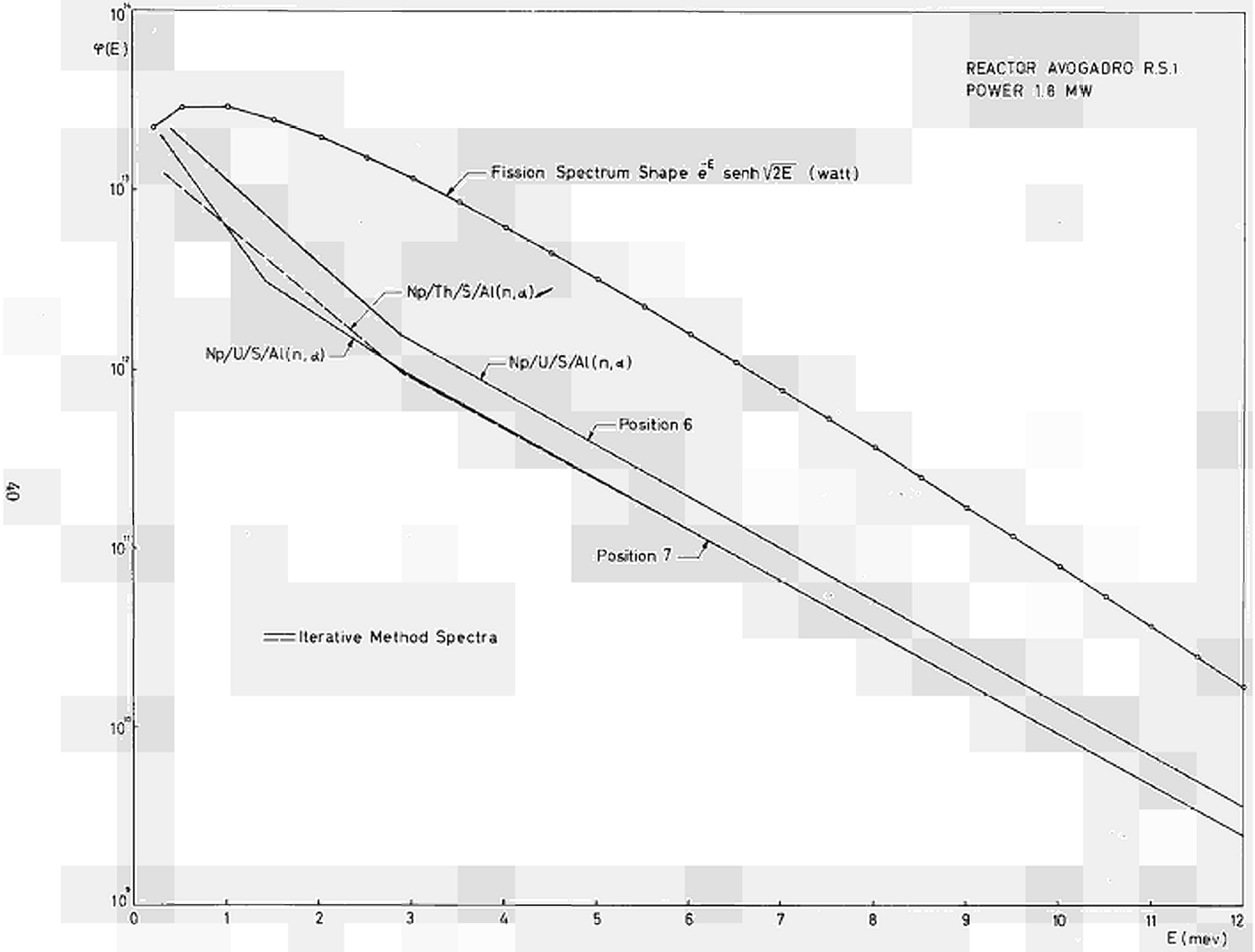


Fig. 17 — Fast neutron spectra

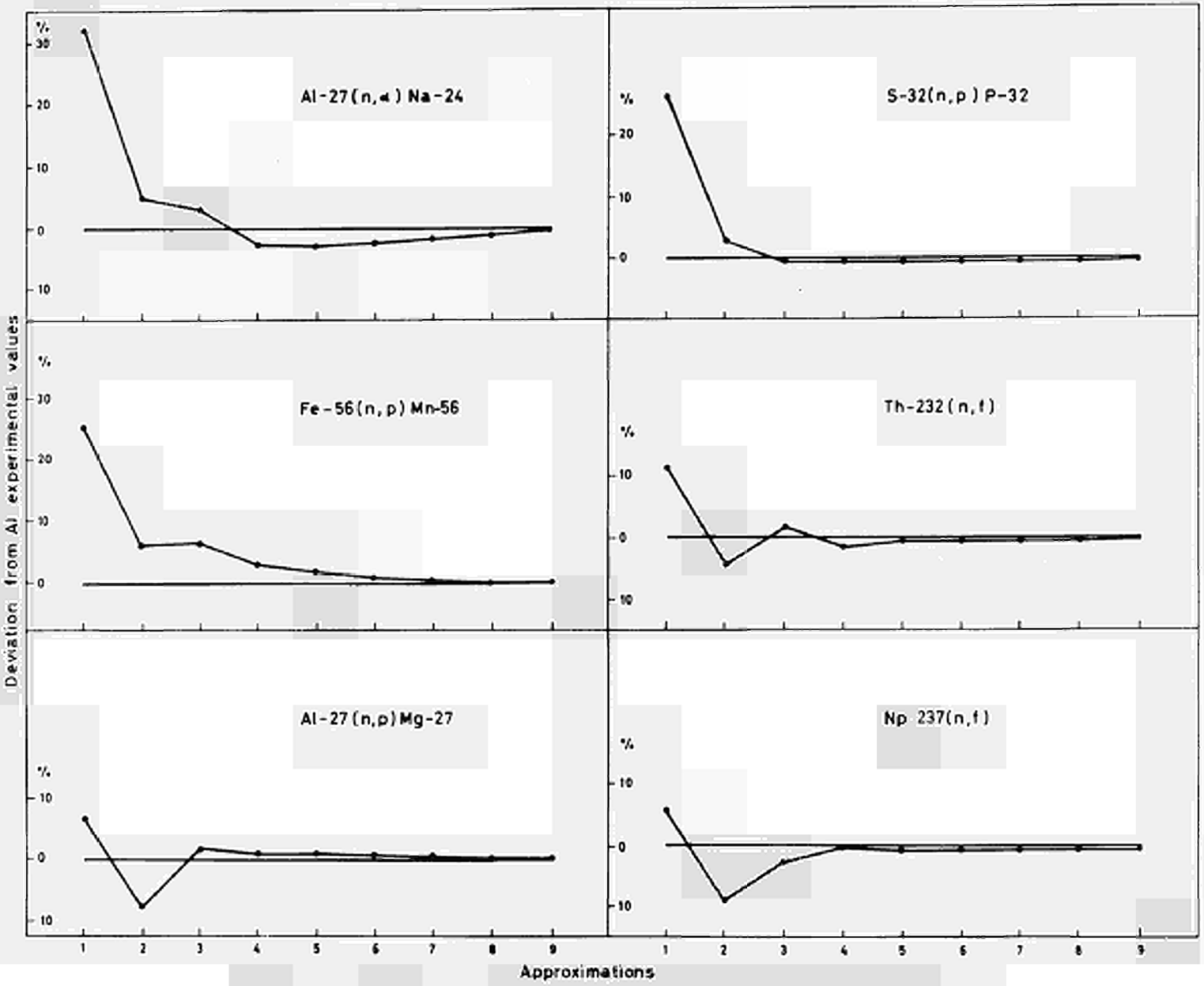


Fig. 18 — Deviation from $A_i$ experimental values in successive approximations

CDNA00289ENC